(4)

David Taylor Research Center

Bethesda, MD 20084-5000

AD-A221 497

DTRC/SHD-1298-04 March 1990

Ship Hydromechanics Department

Departmental Report

INSTALLATION AND PRETEST ANALYSIS OF DARPA SUBOFF MODEL IN THE DTRC ANECHOIC WIND TUNNEL

by

Han-Lieh Liu

Chen-Wen Jiang

David J. Fry

Ming S. Chang

DTRC/SHD-1298-04 INSTALLATION & PRETEST ANALYSIS OF DARPA SUBOFF MODEL IN DTRC AFF

MAJOR DTRC TECHNICAL COMPONENTS

CODE 011 DIRECTOR OF TECHNOLOGY, PLANS AND ASSESSMENT

12 SHIP SYSTEMS INTEGRATION DEPARTMENT

14 SHIP ELECTROMAGNETIC SIGNATURES DEPARTMENT

15 SHIP HYDROMECHANICS DEPARTMENT

16 AVIATION DEPARTMENT

17 SHIP STRUCTURES AND PROTECTION DEPARTMENT

18 COMPUTATION, MATHEMATICS & LOGISTICS DEPARTMENT

19 SHIP ACOUSTICS DEPARTMENT

27 PROPULSION AND AUXILIARY SYSTEMS DEPARTMENT

28 SHIP MATERIALS ENGINEERING DEPARTMENT

DTRC ISSUES THREE TYPES OF REPORTS:

1. **DTRC reports, a formal series,** contain information of permanent technical value. They carry a consecutive numerical identification regardless of their classification or the originating department.

2. **Departmental reports, a semiformal series,** contain information of a preliminary, temporary, or proprietary nature or of limited interest or significance. They carry a departmental alphanumerical identification.

3. **Technical memoranda, an informal series,** contain technical documentation of limited use and interest. They are primarily working papers intended for internal use. They carry an identifying number which indicates their type and the numerical code of the originating department. Any distribution outside DTRC must be approved by the head of the originating department on a case-by-case basis.

REPORT DOCUMENTATION PAGE

1a. REPORT SECURITY CLASSIFICATION: Unclassified	1b. RESTRICTIVE MARKINGS
2a. SECURITY CLASSIFICATION	3. DISTRIBUTION / AVAILABILITY OF REPORT: Approved for public release; distribution is unlimited.
2b. DECLASSIFICATION / DOWNGRADING SCHEDULE	
4. PERFORMING ORGANIZATION REPORT NUMBER(S): DTRC/SHD-1298-04	5. MONITORING ORGANIZATION REPORT NUMBER(S)
6a. NAME OF PERFORMING ORGANIZATION: David Taylor Research Center; 6b. OFFICE SYMBOL (If applicable): Code 1542	7a. NAME OF MONITORING ORGANIZATION
6c. ADDRESS (City, State, and Zip Code): Bethesda, MD 20084-5000	7b. ADDRESS (City, State, and Zip Code)
8a. NAME OF FUNDING / SPONSORING ORGANIZATION; 8b. OFFICE SYMBOL (If applicable)	9. PROCUREMENT INSTRUMENT IDENTIFICATION
8c. ADDRESS (City, State, and Zip Code)	10. SOURCE OF FUNDING

PROGRAM ELEMENT NO.	PROJECT NO.	TASK NO.	WORK UNIT ACCESSION NO.
63569N		S1974030	DN509067

11. TITLE (Include Security Classification)

INSTALLATION AND PRETEST ANALYSIS OF DARPA SUBOFF MODEL IN THE DTRC ANECHOIC WIND TUNNEL

12. PERSONAL AUTHOR(S): Han Lieh Liu, Chen-Wen Jiang, David J. Fry and Ming S. Chang

13a. TYPE OF REPORT	13b. TIME COVERED	14. DATE OF REPORT (Year, Month, Day)	15. PAGE COUNT
Departmental	FROM_____ TO_____	1990, March	51

16. SUPPLEMENTARY NOTATION

17. COSATI CODES			18. SUBJECT TERMS (Continue on reverse if necessary and identify by block number)
FIELD	GROUP	SUB-GROUP	DARPA SUBOFF model assignment; VSAERO-numerical studies tunnel flow condition

19. ABSTRACT (Continue on reverse if necessary and identify by block number)

Detailed flow measurements around an axisymmetric body were required in the wind tunnel as a part of the SUBOFF Program. To ensure the quality of all experimental data, potential flow and boundary layer computer programs were used to determine the effects of tunnel blockage, the supporting struts,the open jet, and the procedure to align the model with the flow in the wind tunnel. The results of these pre-test analyses were then used to guide the experimental setup and tunnel reference velocity selection.

Pre-test analyses indicated that the velocity distribution in the x/L=0.85 plane was quite uniform. It is recommended that this plane should be used as the tunnel reference plane to normalize all predicted and measured velocities and pressures. The majority of tunnel blockage effect is estimated by using these references. The most sensitive locations for the surface pressure measurements were at the pressure taps at x/L=0.04 and 0.78. The pressure variations at these locations were used to align the model with the flow in the wind tunnel.

20. DISTRIBUTION / AVAILABILITY OF ABSTRACT: ☑ UNCLASSIFIED/UNLIMITED ☐ SAME AS RPT ☐ DTIC USERS	21. ABSTRACT SECURITY CLASSIFICATION: Unclassified
22a. NAME OF RESPONSIBLE INDIVIDUAL: Han Lieh Liu	22b. TELEPHONE (Include Area Code): 301-227-1324; 22c. OFFICE SYMBOL: Code 1542

DD FORM 1473, 84 MAR

83 APR edition may be used until exhausted
All other editions are obsolete

CONTENTS

page

ABSTRACT 1
ADMINISTRATIVE INFORMATION 1
INTRODUCTION 1
NUMERICAL STUDIES 3
GENERAL INTRODUCTION 3
BLOCKAGE EFFECT 3
STRUT EFFECT 4
OPEN JET EFFECT 5
VISCOSITY EFFECT 5
WIND TUNNEL 6
MODEL 7
MODEL ALIGNMENT EQUIPMENT DESIGN 8
GIMBAL DESIGN 7
STRUT BASE DESIGN 8
MODEL ALIGNMENT PROCEDURE 8
PHYSICAL ALIGNMENT 9
HYDRODYNAMIC ALIGNMENT 10
MODEL-TRAVERSE-PROBE ALIGNMENT PROCEDURES 12
MEASUREMENT PLANE LOCATED WITHIN THE BODY LENGTH 12
MEASUREMENT PLANE LOCATED OFF THE BODY LENGTH 13
TEST SECTION FLOW CONDITION 14
TUNNEL STATIC PRESSURE AND VELOCITY DISTRIBUTION 14
IN-FLOW AND OUT-FLOW PLANES CONDITIONS 15
REFERENCE VELOCITY SELECTION 15
CONCLUSION 15
ACKNOWLEDGEMENT 16
APPENDIX A: SAMPLE INPUTS FOR VSAERO PROGRAM 41
REFERENCES 51

FIGURES

page

1. Grid Representation of Axisymmetric Hull of DTRC Model 5471 – The Open Flow Model....17
2. Grid Representation of Axisymmetric Hull of DTRC Model 5471 – Inside the AFF Tunnel....18
3. Effect of Tunnel Blockage on the Computed Surface Pressure Coefficients....19
4. Grid Representation of Axisymmetric Hull with Struts Inside the AFF Wind Tunnel....20

5a. Effects of Tunnel Blockage and Two Supporting Struts on the Computed Inviscid Surface Velocity, at $\theta = 139°$....21

5b. Effects of Tunnel Blockage and Two Supporting Struts on the Computed Inviscid Surface Velocity, at $\theta = 155°$....22

5c. The Effect of Struts on the Circumferential Distribution of Surface Potential Flow Velocities....23

6. The Strut Wakes Estimated by Two-Dimensional Approximation....24
7. Grid Representation of Axisymmetric Hull in a Circular Tunnel....25
8. *Effect of Jet Region on* Computed Surface Pressure Coefficients....26
9. Effect of the Tunnel Blockage on the Computed Surface Pressure Coefficients of a Displacement Model 5471 Normalized with U_{ref} at $x/L = 0.85$....27
10. Comparison of the Measured and Computed Static Pressure Distribution along the Model, normalized with U at $x/L = 0.85$....28
11. Comparison of Measured and Computed Velocities along the Tunnel Axis, normalized with U at $x/L = 0.85$....29

12a. Computed Off-Body Velocities Inside the AFF....30

12b. Computed Off-Body Velocities – Infinite Fluid....31

13. Model Setup Inside the AFF Wind Tunnel....32
14. Gimbal Assembly....33
15. Strut Base Design....34
16. Effect of Model Alignment on Computed Surface Pressure Coefficients....35
17. Tunnel Velocity Survey along the Ceiling with and without Model, normalized with U at $x/L = 0.85$....36
18. Tunnel Static Pressure Survey along the Ceiling with and without Model....37
19. Tunnel Static Pressure Computations and Measurements along the Ceiling Centerline....38

TABLES

page

1. Measured Model Radius Offsets (Anechoic Flow Facility Model Nos. 5470 and 5471).....39

NOMENCLATURE

C_p	static pressure coefficient
L	model length
P_o	free stream static pressure
P_{ref}	tunnel reference pressure at $x/L = 0.85$ and $r/R_{max} = 3.6$
r	radial position from the model centerline
R_{max}	model body radius
U_e	local velocity at the boundary layer edge
u_b	potential flow surface velocity without strut effect
u_s	potential flow surface velocity with strut effect
u_x	axial velocity component
U_o	free stream reference velocity
U_{ref}	tunnel reference velocity at $x/L = 0.85$ and $r/R_{max} = 3.6$
X	streamwise coordinates (positive downstream)
Y	transverse coordinates (positive outbound)
Z	vertical coordinates (positive vertical upwards)

ABBREVIATIONS

AFF	Anechoic Flow Facility Wind Tunnel
CFD	Computational Fluid Dynamics
DARPA	Defense Advanced Research Project Agency
DTRC	David Taylor Research Center
STP	Submarine Technology Program
SUBOFF	Submarine Flow Field
VSAERO	Computer Program for Calculating the Nonlinear Aerodynamic Characteristics of Arbitrary Configurations

ENGLISH/SI EQUIVALENTS

1 foot	=	0.3048 m (meters)
1 foot per second	=	0.3048 m/s (meters per second)
1 inch	=	25.4 mm (millimeters)
1 lb (force)	=	4.488 N (Newtons)
1 lb(force)-inch	=	0.113 N - m (Newton - meter)
1 long ton (2240 lbs)	=	1.016 metric tons, or 1016 kilograms
1 horsepower	=	0.746 KW (kilowatts)

ABSTRACT

Detailed flow measurements around an axisymmetric body were required in the wind tunnel as a part of the SUBOFF Program. To ensure the quality of all experimental data, potential flow and boundary layer computer programs were used to determine the effects of tunnel blockage, the supporting struts,the open jet, and the procedure to align the model with the flow in the wind tunnel. The results of these pre-test analyses were then used to guide the experimental setup and tunnel reference velocity selection.

Pre-test analyses indicated that the velocity distribution in the x/L=0.85 plane was quite uniform. It is recommended that this plane should be used as the tunnel reference plane to normalize all predicted and measured velocities and pressures. The majority of tunnel blockage effect is estimated by using these references. The most sensitive locations for the surface pressure measurements were at the pressure taps at x/L=0.04 and 0.78. The pressure variations at these locations were used to align the model with the flow in the wind tunnel.

ADMINISTRATIVE INFORMATION

This work was performed at the David Taylor Research Center (DTRC) in Bethesda, Maryland 20084-5000. The project was funded by DARPA, Task Area S1974-030, Program Element No. 63569N with internal DTRC Work Unit Numbers 1542-123, 1542-126 and 1542-127.

INTRODUCTION

The Submarine Technology Program (STP) Office of DARPA funded a coordinated Computational Fluid Dynamics (CFD) Program to assist in the development of advanced submarines for the future. This DARPA SUBOFF project will provide a forum for the CFD community to compare the numerical predictions of the flow field over an axisymmetric hull with and without various appendages with experimental data. The results of these comparisons can then be used to demonstrate the current CFD capability on design problems relevant to the STP problem area.

Since the objective of this experiment was to provide accurate data for code validation, extra care with data quality was demanded. At the outset of the entire test program it was necessary to define the wind tunnel flow condition for reference. It was also necessary to define various alignment procedures to standardize the model setup for various test conditions. Pretest analysis of the tunnel flow over a strut-mounted model was then conducted to provide guidance.

The equations and models to define the axisymmetric body, fairwater, stern appendages, ring wings and supporting struts were detailed in reference [1]. Eight model configurations were selected for the experimental and computational SUBOFF programs [2]. They were

(1) a bare axisymmetric body;
(2) an axisymmetric body with a fairwater;
(3) an axisymmetric body with four identical stern appendages;
(4-5) an axisymmetric body with fairwater at angle of attack or drift;
(6-7) an axisymmetric body with two different stern ring wings; and
(8) an axisymmetric body with fairwater and four baseline appendages.

For the present pre-test analysis, however, computations were done on only the bare axisymmetric body represented by DTRC Model 5471 mounted in the tunnel.

Two computer codes were used: the VSAERO [3] and the modified Douglas Cebeci-Smith boundary layer program [4,5]. The VSAERO program was used to define the tunnel flow condition; the effects of model blockage; the effects of supporting struts and open jet; and the pressure variations across the model cross sections due to the angle of attack of the model. The boundary layer program was used mainly to define the displacement thickness of the axisymmetric body. The resultant axisymmetric body was then used by the VSAERO program to calculate the surface pressure distribution and alignment requirements.

This report briefly describes the numerical pre-test studies; the wind tunnel used in the test program; the model used in the actual tests; the model alignment procedures; the model-traverse-probe alignment procedures; the in-flow and out-flow conditions to the model in the wind tunnel; and the selection of the reference velocity and pressure.

NUMERICAL STUDIES

GENERAL INTRODUCTION

The panel code computer program VSAERO, was used to simulate the flow field in the AFF. The fairwater and the stern appendages were not modeled in this numerical model because the study was not intended to provide the detailed flow distribution. The tunnel flow with the open jet section, the viscous effect, and the tunnel blockage effect were estimated first for the bare axisymmetric body before using a more complicated model representation (i.e. a model with struts). The numerical model was then expanded to include the struts for estimating the strut influence on the flow around the body. Due to the fact that the model stern had to be installed in the open jet section of the AFF wind tunnel, it was necessary to determine the effect of the tunnel open jet on the flow over the body. The last part of this section estimates the viscous effect.

BLOCKAGE EFFECT

To assess the tunnel blockage effect, i.e. with and without the tunnel wall, two computations were performed for the cases where the bare model was placed in the closed tunnel and in an infinite fluid. The results of these computations demonstrated the model blockage effect in the wind tunnel. Figure 1 depicts the grid representation of the axisymmetric model. The two dense grid regions are the positions where the struts are located in the closed tunnel. Figure 2 represents the model in the AFF tunnel with the inlet at 1.52 m (5 ft) ahead of the bow and the outlet at 1.44 m (4.71 ft) after the stern of the model. A uniform flow field was assumed at the inlet and the outlet. Appendix A is a listing of model data sample input for the VSAERO program.

Figure 3 is the pressure coefficient distribution along the DARPA model in an infinite fluid and in the AFF tunnel. The differences between these results represent the blockage effect in the AFF tunnel due to the presence of the model. As shown in Figure 3, the overall tunnel blockage can be estimated as the average difference in the values of C_p over the body length. This difference in C_p is about 0.05 and hence the difference in velocity is about 0.025. This is about the same order as the error in velocity measurements along the tunnel to be discussed in Figure 17.

STRUT EFFECT

Two identical NACA-0015 struts were used to support the model at x/L = 0.24 and 0.63. The chords of these struts were 15 cm (6 inches). Most of the measurements were made for the flow on the upper surface of the model where strut effects were minimal. In order to support this argument, two struts were modeled in the VSAERO calculation. The grid representation of this inclusion is shown in Figure 4. The effects of the model blockage and the two struts on the computed inviscid surface velocities along the body are given in Figures 5a and 5b for the two different angular positions: 139° and 155°, respectively. The angle is measured from the vertical plane counterclockwise from the top as viewed from the stern to bow. The circumferential distributions of velocity perturbations with and without the two support struts were estimated by VSAERO computer code at x/L= 0.621, 0.691, 0.840 and 0.978. The computed potential-flow surface velocities (u_s), with and without the struts, over the hull at x/L=0.621 are shown in Figure 5c. This figure represents the maximum disturbance from VSAERO calculation. The disturbance from the struts on the axisymmetric body is shown in the immediate area of the strut.

The strut disturbances decay very fast downstream. At x/L=0.621, the velocity disturbance from the strut $(u_s - u_b)/u_b$ is less than 0.3% at 170°, and 0.1% at 135°, where u_b is the potential-flow surface velocity without the strut effect.Further downstream from the struts at x/L=0.840 and 0.978, the computed potential-flow values of $(u_s - u_b)/u_b$ are less than 0.004%. However the viscous wakes of the struts may be more significant in these locations. The estimated viscous flow disturbance from the struts was calculated from Cebeci-Smith's boundary layer computer program [4, 5] and is shown in Figure 6 to be limited to the immediate strut area for five x/C locations, where C is the strut chord length and U_e is the boundary layer velocity based on boundary layer thickness at the corresponding axial location. The computed variations of axial velocities on the body are very small and the strut wake decays rather quickly. After about four chord lengths downstream of the strut the wake is only about 5% of U_e. The width of the wake is only a fraction of the chord. Therefore the strut-wake influence region is limited to the immediate area of the strut. The measurements on the upper part of the body should not be disturbed by the underside struts. In the actual test setup, due to the interaction of the strut wakes and the boundary layers on the hull a somewhat larger strut wake is expected. A more complete analysis of the effect of the strut wake on the model using a Reynolds-averaged Navier-Stokes simulation will be presented in a separate report.

OPEN-JET EFFECT

There was some concern about the open-jet region near the stern of the model in the AFF tests. More precisely, the forward section of the model was in the closed tunnel section while the model stern extended into the open jet section of the tunnel. This arrangement was necessary due to the relatively large size of the model. To estimate this effect, a free surface boundary condition was assumed in the tunnel jet region to predict the pressure coefficient along the model. Velocity components in the flow direction on the panels of the open-jet region were iterated to achieve a constant value by imposing different normal velocities on the tunnel panels in the open-jet region. In order to simplify the iteration procedure, an equivalent circular area of the tunnel was used in the computation. Both the model and the tunnel were axisymmetric so that the free surface was also axisymmetric. The panel representation of the model and the tunnel is shown in Figure 7. The last one third of the tunnel panels had normal velocities specified in the VASERO calculation to iterate for the free surface boundary condition. Figure 8 demonstrates that the jet region has a relatively small influence on the surface pressure calculation near the stern. The open jet flow tends to locally follow earlier open flow condition calculations.

Since only a small portion of the model was in the open jet and the computed effect of the free surface of the open jet on the values of C_p was small, further simulation of the open jet was not deemed necessary.

VISCOSITY EFFECT

Since viscous effects are important in the model stern region, the numerical model was then modified to include the boundary-layer displacement thickness computed from the modified Douglas Cebeci-Smith axisymmetric boundary layer program [4,5]. A modified axisymmetric body based on the calculated displacement thickness was then used for various flow quantity calculations. Figure 9 shows the surface pressure coefficients along the displaced DARPA model. Two reference velocities were used in the pressure coefficient calculation, one was the uniform inflow velocity and the other was the velocity at the plane x/L = 0.85. The computed velocities at this x/L location were uniform across the entire plane except the area blocked by the model, and were equal to the free stream velocity for the case of flow without tunnel wall effect and equal to 1.024 times the inflow velocity for the case of the tunnel wall effect. It is also interesting to observe that the

pressure coefficients, based on the reference velocity and pressure at x/L = 0.85, are very close to each other for either condition: with or without the tunnel wall in the computation. Thus, the tunnel blockage effect can almost be eliminated by using the reference velocity and pressure at x/L=0.85.

This simple numerical displacement model has been used to define the overall blockage effect of the AFF tunnel. The rest of the numerical studies presented below are thus based on this displacement model approximation.

Figure 10 presents a comparison of the surface static pressure distribution for the AFF measurements and the numerical prediction. Except for the sharp pressure gradient occuring near the nose region, the comparison between the measured and computed values of C_p is quite favorable. A comparison of measured and computed velocity profiles along the tunnel is presented in Figure 11 for three radial distances. The simple numerical displacement model simulates the potential flow inside the tunnel very satisfactorily. The velocity changes along the tunnel, due to the combination of body and tunnel effects at the three foregoing radial locations are depicted in Figure 12a. It may be seen that the calculated axial velocity component is uniform at the plane x/L=0.85 where the value of u_x/U_o is equal to 1.024. This represents the overall tunnel blockage effect. A further check of this reference location was carried out with computations of the model in the open flow condition. Again, the three velocity profiles cross over at about the same x/L location (Figure 12b). This plane is thus recommended as the reference plane for the experiments.

WIND TUNNEL

The wind tunnel used for the present SUBOFF Program is the Anechoic Flow Facility (AFF) [6] of the David Taylor Research Center (DTRC). The tunnel is a reinforced concrete, horizontal circuit of square cross sections with corner fillets. The air in the tunnel is moved by a fan around a closed loop emerging from a nozzle in which the stream is contracted from an area of 54.348 m^2 (585 sq. ft.) to an area of 5.426 m^2 (58.4 sq. ft.). The air passes through the closed test section into the anechoic chamber and then successively through various diffusers and mufflers to minimize the noise and the turbulence generated in the flow loop and by the fan.

The test section has a 2.439 m (8 ft) square cross section with fillets of 0.534 m (1.75 ft) in each corner. The test section is 2.718 meters (8.917 ft) long. Allowance for boundary layer growth along the tunnel is made by slightly tapering the fillet in the test section walls

so that there is no effective contraction of the flow and no resultant pressure gradient along the test section. To obtain the required rate of area expansion, the 0.534 m (1.75 ft) fillets are tapered, starting at the test section entrances, by 0.00273 m per 0.3048 m (0.00897 ft per ft) of run to 0.509 m (1.67 ft) on the side at the test section exit. The test section configuration is shown in Figure 13.

The air speed monitored during the test was determined from the measurement of the pressure differential across the 'contraction'. Two manifolded rings of surface pressure taps served as venturi taps to furnish differential pressure readings on a connected micromanometer. Due to daily changes in barometric pressures and tunnel operating temperatures, this differential pressure was held constant at all times to yield a nominal Reynolds number of twelve million (based on the body length).

MODEL

The model used in the actual tests is constructed of molded fiber glass shell and reinforced with a 10-inch wide U-channel as its strongback. Due to the requirement that the fairwater would be rotated 90-degree with respect to its centerline as one of the test conditions, the seam lines for the two halves of the shells were offset. The finished model was checked for the smoothness of the surface finishing.

The measurements of physical radii of the model at selected axial locations were conducted in the DTRC model shop. The model was positioned on the flat model layout table and the center of the model axis was defined. A true carpenter square was used to move along the table for various radius measurements at different axial locations. The model was rotated about its axis every 45° for the measurements of the radii at the same axial location. Ten readings for each station were taken and the standard deviation of the measurements was computed. The results are tabulated in Table 1. The largest difference in measurements occur in the seam area. As much as 0.1 inch (2.5 mm) was observed in the nose area and the stern area with a standard deviation of 0.05 inches in measurements. A much better construction along the parallel mid body had a standard deviation of less than 0.03 inches. The average radius was much closer to the design requirements. The impact of this 'not too axisymmetrical' nose on the final flow development over the body was considered to be not serious because most of these 'bad' spots occurred before the trip wire from the nose. The body should be experiencing a fully developed turbulent flow after the trip wire. For all practical purposes, it was assumed that the impact was small.

MODEL ALIGNMENT EQUIPMENT DESIGN

The model was supported by two thin NACA0015 struts. They were in turn mounted on the strut bases below the floor for minimal flow disturbance. Two 1/16-inch cables were attached to either side of the strut and anchored to the tunnel wall for model stability. The model end of the strut was connected to a gimble which was secured to the model strong back. The gimbal arrangement and the strut base design allowed the degrees of freedom required to align the model for various configurations. A brief discussion of the designs follows.

GIMBAL DESIGN

In the test plan, the model was required to pitch and yaw two degrees in either direction. Since any model change inside the wind tunnel is always time consuming, two gimbals were mounted on the model strong back for the two supporting struts to facilitate this model configuration change. The two axes of the gimbal were in the model pitching plane and the yawing plane, Figure 14. For pitching, the rear strut was lowered in the rear strut base to the desired location while the front strut was held fixed. To achieve the model yaw angles, either the rear strut or both the front and the rear struts were moved horizontally on the strut bases. Both struts were still kept in line to the flow at all time. It was anticipated that serious strut wakes might result under the yaw test conditions since the two struts were not along the same flow line.

STRUT BASE DESIGN

One of the design requirements for the strut and its base was to generate minimal flow disturbance. To achieve this, it was decided that the strut base should be supported below the tunnel floor. Adjustment screws were incorporated on the base to align the base to the model and the tunnel. Figure 15 shows the sketch of this base and its adjustment bolts.

MODEL ALIGNMENT PROCEDURE

Wind tunnel models are typically aligned with the tunnel geometric axes, i.e. matching the tunnel centerline with the model centerline. This will be referred to as a "physical alignment". However, from previous experiments, it has been noted that the tunnel flow does not remain exactly aligned to the tunnel centerline once the model is installed. This is because the model and its supporting structures, cables or struts, create a

blockage effect. Ideally, it is preferred to support the model with cables only for which a minimal blockage can be achieved. Once the struts are attached to the model, the flow over the model cannot be said to be entirely axisymmetric due to the unbalanced strut blockage. This may be one of the reasons that the flow axis does not match the tunnel axis once a model is installed inside the tunnel test section. A hydrodynamic alignment of the flow to the model is therefore needed if axisymmetric flow over the body is required.

The cable arrangement was abandoned because the cables generate turbulence and the three flow turbulence velocities were variables to be measured. The turbulence generated by the strut is believed to be limited only to the immediate area around the strut as discussed earlier. The strut is therefore the preferred method of support. The use of one large strut support versus two-thin strut supports was debated. The two-thin strut supports were selected because they had less blockage effect. This section discusses the procedure involved to properly align a two-strut supported model in the wind tunnel test section.

PHYSICAL ALIGNMENT

In order to establish baseline information on the model alignment to the flow, the model centerline was first aligned to the tunnel centerline. This alignment was conducted with the help of a surveyor's transit located 10 m (32.8 ft.) downstream from the end of the model. The steps involved were:

1. Define the tunnel centerline at the test section and at the transit location: two control points were previously marked, one at the floor I-beam under the test section and one at the tunnel downstream section. They were located on the tunnel centerline. The transit was set up at the downstream mark and adjusted to sight the test section center mark. This procedure aligned the transit with the tunnel physical axis..

2. Place the bow on the tunnel centerline: a point on the model near the bow was needed for bow alignment. The pressure taps used for the surface pressure measurements defined a meridian line along the model top (where a vertical plane through the model longitudinal axis meets the model surface). A V-block was first aligned to the model meridian line directly above the forward strut. A flag on the V-block centerline was easily sighted by the transit. The model forward strut was adjusted to make sure the bow was on the tunnel centerline as viewed from the transit. When the bow was centered, the anchoring bolts on the

forward strut base were secured.

3. Align the model stern to the tunnel centerline: the surface pressure tap at the end of the model provided a convenient spot for visual alignment by the transit. With the help of the gimbal from the forward strut, the whole model could be rotated around the gimbal vertical axis without imposing any torque on the model. The rear strut and its base were adjusted to the desired location – in line with the tunnel centerline.

4. Revisit previously established bow alignment: it was necessary to assure the bow and the stern of the model remained in-line with the tunnel physical center plane after the stern adjustment. The locking bolts on the rear strut base were secured when both bow and stern were aligned. The model was now yaw-adjusted to the tunnel centerline.

5. Determine model pitch : the model center at the nose was first establised. Since this point was not visible to the transit, an extension bar was used to horizontally transport this nose center location off from the body to a convenient location visible to the transit. An adjustable height table and machinists' level were used for this task.

6. Adjust the rear strut vertical motion to align the model stern to the same level as the nose center. It was found that the model was level in pitch angle. No shim was necessary for any adjustment.

This completed the model physical alignment to the tunnel with respect to its pitch and yaw angles.

HYDRODYNAMIC ALIGNMENT

After the model was physically aligned with the tunnel, a dynamic test of the flow around the model was conducted by measuring pressures around the body circumference at the same axial location. For an axisymmetric body, the pressure around the body circumference should be identical. Differences in pressure measurements between the upper and lower surfaces could indicate that the model was pitched. Similarly, differences in the starboard and port side of the body could reveal the misalignment in the yaw direction. The dynamic alignment procedure measured the pressures in four circumferential locations on the body at the same x/L. Strut positions were adjusted until

the four readings matched. The present model has pressure taps on the port/starboard and upper/lower surfaces in several axial locations. These pressure tap "rings" were used to check the flow around the model at various axial locations.

The first pressure ring was located forward of the model trip-wire. This was the location where the flow begins to develop along the model and does not experience strut interference. However, since these pressure taps are located very close to the model nose, the boundary layer is still in the developing stage. The sensitivity was not considered adequate. Two more rings were considered to complement the data from the first ring. The second ring was located at the mid body and the third ring was located toward the stern but before the body cross-section begins to decrease. In examining the surface pressure calculation over the axisymmetric body, it was clear that the second ring was still inadequate for the present alignment purpose – the pressure there was too small in magnitude. The resolution was poor. The surface pressures at the third ring axial location had considerably larger values and it was on the rising part of the pressure curves. It thus provided a more sensitive location for alignment. This location, at $x/L = 0.781$, was thus chosen for flow alignment studies. It should be pointed out that the model body at this location, i.e. its radius, was also smooth and close to the design model radius, (refer to the model offsets in Table 1).

The VSAERO potential flow code was used to calculate the variation of surface pressure changes due to different angles of attack of the model, Figure 16. These theoretical predictions provided the guideline for adjusting the struts to obtain minimal differences among the pressure taps at a given axial location. Pitch angle sensitivity, change of C_p versus changes in pitch angle, is then derived from these curves as a guideline for dynamic alignment. The model adjustment during this phase was concentrated at the rear strut only. After the strut was adjusted according to the guideline, the pressure measurement was repeated to verify the changes made. Typical pressure measurement results are shown for an aligned model in the following table:

Tap Number	C_p
HU12	0.229594
HP12	0.221735
HS12	0.223718
HL12	0.222502
VSAERO	0.222700

where H stands for the hull pressure tap defined in Reference 1 and U, P, S, and L for the upper, port, starboard and lower surfaces on the model, respectively. The number 12 indicates the pressure tap at station 12 which corresponds to x/L=0.781. To achieve this dynamic alignment, the model required a physical alignment of 0.00 degree pitch angle and about 0.15 degree yaw angle (to the starboard with respect to the tunnel geometric axis). The angle between the geometric center of the tunnel and the model axis after this dynamic alignment is 0.15 degree. The accuracy of aligning the model in a large wind tunnel by the present procedure is about the same order of magnitude. Thus an overall accuracy of model alignment with the flow should be of the order of 0.2 degree or less.

As a result of this dynamic alignment, the rear strut had to be moved toward the port side by 10 mm (0.25 in). Although these two struts were in-line to the flow, their chord centerlines were not matched. Consequently, the strut wakes were interacting and created an anti-symmetrical resultant body wake in the strut area. Special attention should be given to interpolating the data for the body wake behind the struts.

MODEL-TRAVERSE-PROBE ALIGNMENT PROCEDURES

Once the model was properly aligned, the next step was to ensure that the probe and the traverse mechanism were aligned to the model centerline. Two different techniques were employed to align the traverse mechanism for the two different test configurations: the measurement plane was within the model length, ($x/L < 1$), and that the plane was outside the model body length ($x/L > 1$).

MEASUREMENT PLANE LOCATED WITHIN THE BODY LENGTH

The following steps were used to line-up the traverse/probe/model.

a. Position an alignment laser near the model nose area and align the laser beam with the model center line through the help of the pressure taps along the model surface. This procedure fixed the laser beam and the model in the same yaw plane.

b. Mount a V-block with the flag (same V-block used in the previous model alignment) on the far-end of the cylinder on top of the traverse table directly above the adjustment cables.

c. Tighten or loosen the far-end cables attached to the traverse table in order to bring the V-block flag in with the laser beam.

d. Move the V-block to the near-end of the cylinder and repeat step (c) with a second set of adjustment cables. The traverse table centerline was now in-line with the laser and therefore, in-line with the model centerline in the yaw plane.

e. Move the traverse/probe table to the desired x/L location for pitch alignment. It was necessary to align each x/L plane individually because each x/L location had different amounts of traverse overhanging weight. Changes in overhanging weight caused small but measurable changes in the pitch of the traverse rotational axis.

f. Use the model body centerline, a convenient pressure tap at the end of model was used, to align the traverse rotational axis. Four points at 0, 90, 180 and 270 degrees were used to check if the model center matched with the traverse rotational axis. This completed the traverse alignment. The next step was the probe alignment.

g. Mount the probe, (pressure probe, X-wire or three-component wire), on the probe holder. The location of the probe holder was set such that the probe should be in line with the traverse axis aligned earlier. However, a final check of the probe orientation was necessary to ensure its alignment to the model axis.

h. The laser beam of step (a) was used again to determine probe position. The probe was traversed until its sensor was centered in the laser beam. This traverse location was defined as "0" theta angle. The traverse radial location of R_{max} could also be checked. This completed the probe alignment with respect to the model axis.

MEASUREMENT PLANE LOCATED OFF THE BODY LENGTH

The same steps as discussed previously were used except step (f). It would be difficult to use the model body for any alignment reference. A small laser was mounted on the probe holder pointing to the model. The reference points on the model, such as the pressure taps, were used to mark the location of the laser beam as it rotated from 0°, 90°, 180° and 270°. If all four locations on the model were within the measurement tolerance, the axes for the traverse table and the model were aligned.

TEST SECTION FLOW CONDITION

After the model was aligned hydrodynamically, a series of preliminary tests were conducted to check the computer prediction and to provide the flow conditions around the model in the wind tunnel. This included the tunnel's static pressure and velocity distribution along the tunnel centerline at several radial locations, r/R_{max} and the in-flow and out-flow plane conditions.

TUNNEL STATIC PRESSURE AND VELOCITY DISTRIBUTION

A C-Channel was installed on the tunnel ceiling centerline. A trolley could be operated inside the channel and was controlled by the Compumotor. It provided the base for attaching the pitot probes for either static pressure or speed measurements. The pressure lines connected to the pitot probe were run along the track and hung from the ceiling in the anechoic chamber. A weight was attached to these pressure lines in order to straighten these lines under the wind load. Because of this, the trolley could be operated effectively only in the direction from the bow to the stern. The distance it traveled was controlled by the steps set on the Compumotor Indexer. Visual inspection of the actual distance the trolley moved was monitored during the test.

The pitot probe was attatched to the trolley at three r/R_{max} locations: close to the ceiling; close to the model; and in-between (r/R_{max} = 3.6, 2.7, and 1.9). For the empty tunnel case, the measurement was made only at the r/R_{max}=3.6, i.e., close to the ceiling. Figure 17 shows the velocity distribution along the test section inside the tunnel with and without the model. A small velocity gradient is observed. Figure 18 shows the static pressure distribution under the same condition, i.e. with and without the model. A pressure gradient is also observed along the tunnel. Thus for the empty tunnel the measured static pressure coefficient gradient, mainly due to the viscous friction, is found to be 0.003 per foot of the model length in the closed jet test section. However, the measured nondimensional tunnel velocity $u(x)/U_{ref}$ gradient is less than 0.002 per foot of model length for $x/L < 0.7$. The velocity variation is negligible at the stern section where x/L is > 0.7.

For the pressure and velocity surveys along the model at three radial locations, Figure 11 shows the velocity survey discussed earlier and Figure 19 shows the static pressure distributions. Figure 19a shows the computed values of C_p using the VSAERO program where no pressure gradient is imposed in the computation. Figure 19b is the

measured static pressure coefficients. A difference of the computed and measured values is demonstrated. This disagreement is due to the existence of the static pressure gradients in the tunnel. When the tunnel static pressure gradient is subtracted from the actual tunnel test data as shown in Figure 19c, the resultant static pressure distributions match very close by to the VSAERO computer prediction, Figure 19a.

IN-FLOW AND OUT-FLOW PLANES CONDITIONS

The in-flow plane may be selected at $x/L = -0.45$, where there is no difference in the computed axial velocities with and without the model in the tunnel.

The out-flow plane may be selected at $x/L = 1.2$, where the difference in measured axial velocities with and without the model in the tunnel is on the order of 0.5%.

REFERENCE VELOCITY SELECTION

The wind speed and the tunnel static pressure varied along the body and to some extent in the radial direction. It is therefore necessary to designate a location where uniform speed in the cross-section and least sensitive static pressure are expected. After consulting the theoretical prediction of the flow for the body inside the tunnel using the VSAERO code and Figure 19, two pitot probes were mounted at $x/L = 0.85$ and $r/R_{max} = 3.6$. The typical velocity survey at this plane of $x/L = 0.85$ reveals a variation in speed of less than 1% and the static pressure coefficient is close to zero. The velocity at this location is thus called as the tunnel reference free stream velocity. The static pressure at this location is the tunnel reference static pressure to be used for all pressure measurements.

CONCLUSIONS

Pre-test analyses of the flow inside the wind tunnel were carried out before the actual DARPA experimental program began. A simplified numerical model was shown to predict:

(1) the sensitivity of the flow angle (apparent angle of attack) to the model for the dynamic alignment of the model in the existing wind tunnel: The model required a 0.15 degree yaw adjustment.

(2) the effect of the strut on the wake data: It confirmed the assumption that the upper part of the wake data should be free from the strut wake contamination.

(3) the effect of the closed and open jet arrangement of the model in the wind tunnel: This effect was found to be minimal.

(4) the tunnel reference velocity and reference pressure should be placed at x/L = 0.85 and r/R_{max} = 3.6.

(5) in-flow plane with uniform axial velocities may be selected at x/L= -0.45 and the out-flow plane with uniform axial velocities may be assumed at x/L=1.20.

ACKNOWLEDGEMENTS

The authors would like to thank Dr. Thomas T. Huang, for directing this project and Mrs. Nancy C. Groves and Mr. Scott Gowing for their contribution to and participation in the project.

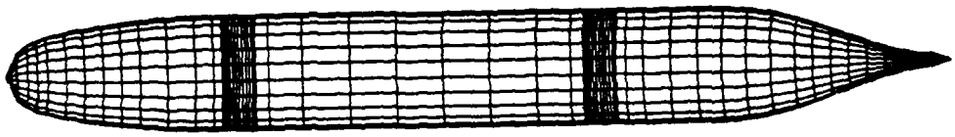

Figure 1 - Grid Representation Of Axisymmetric Hull Of DTRC Model 5471 - The Open Flow Model

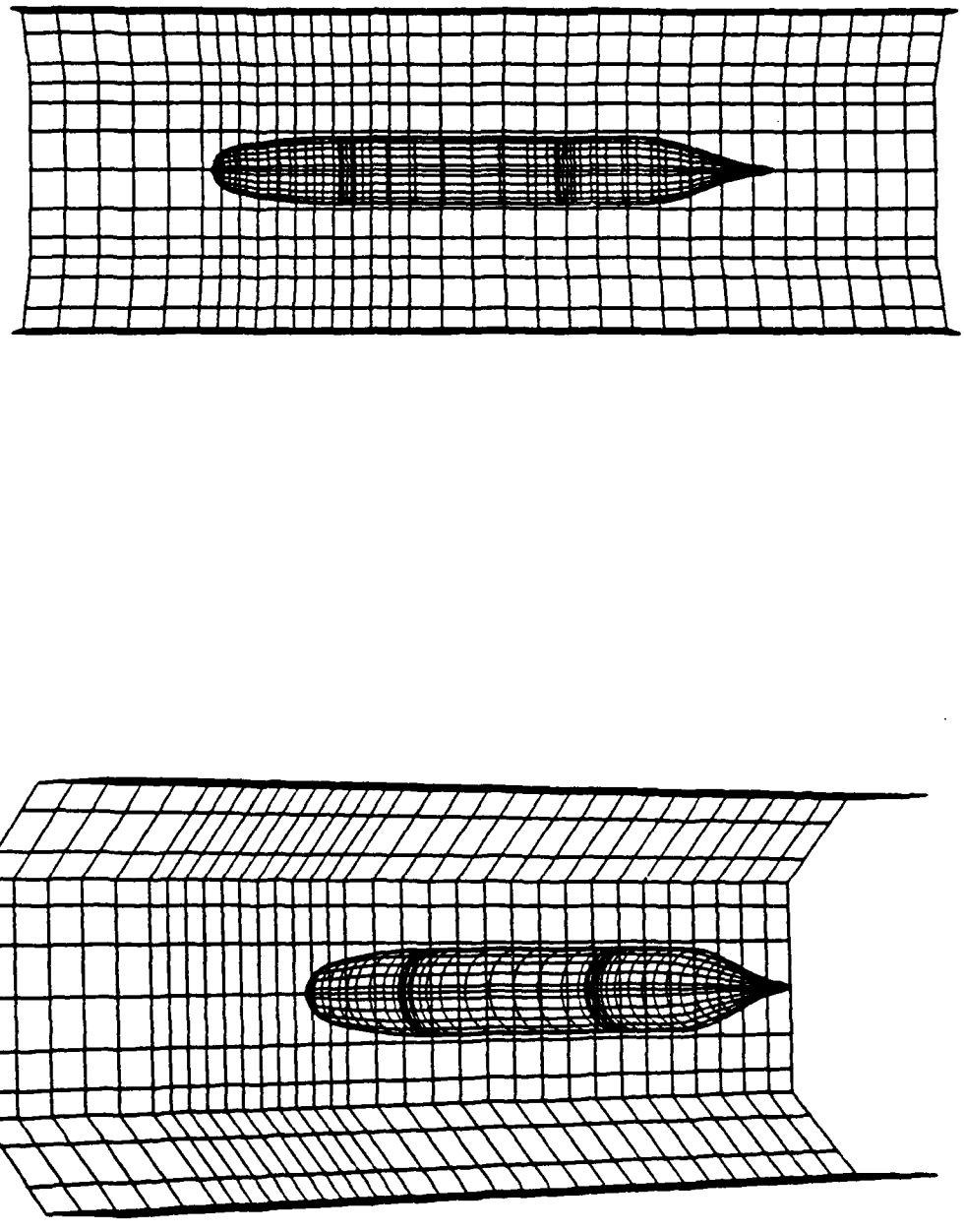

Figure 2 - Grid Representation Of Axisymmetric Hull Of DTRC Model 5471 Inside The AFF Tunnel - The Internal Flow Model

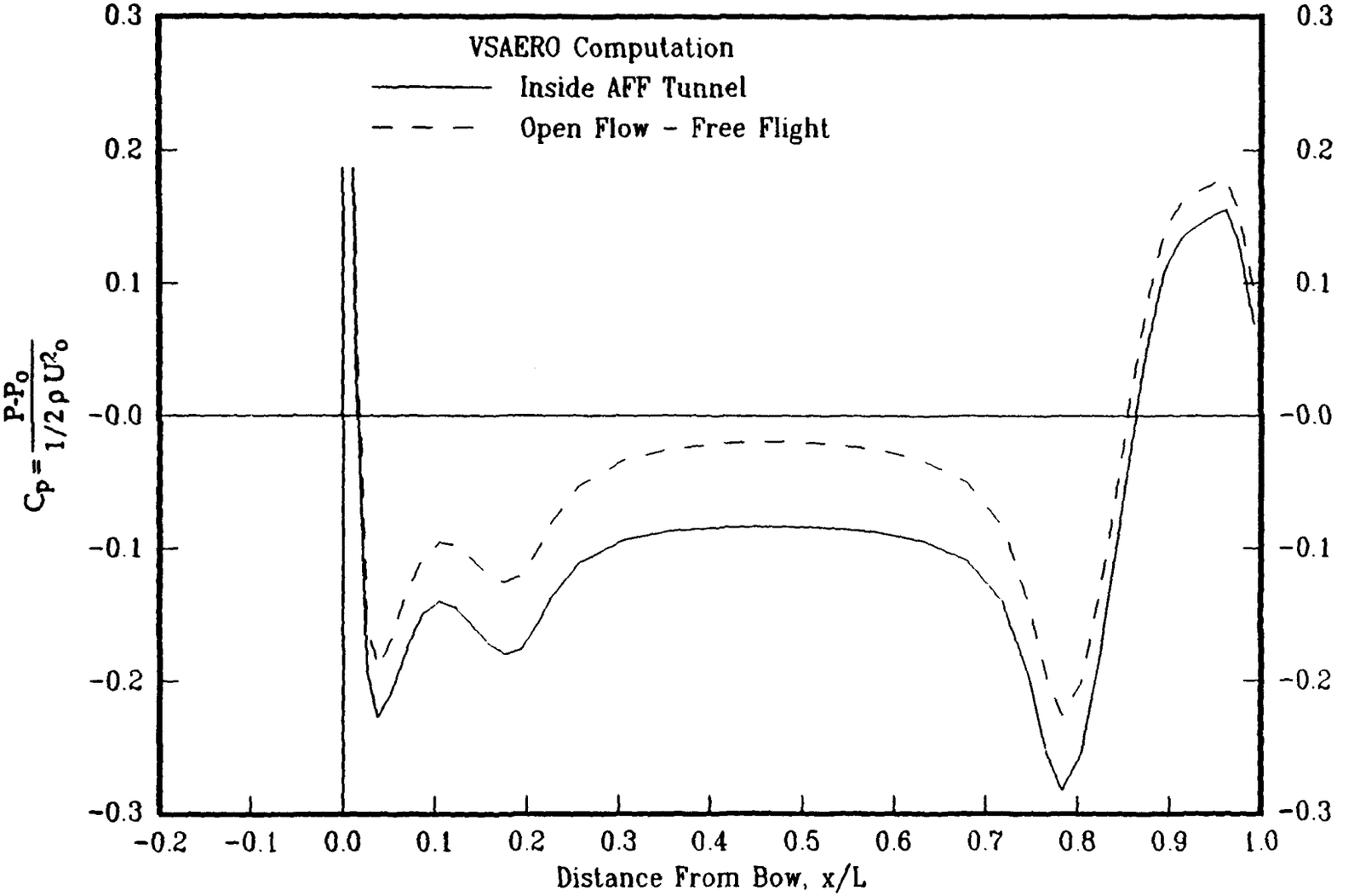

Figure 3 - **Effect Of Tunnel Blockage On The Computed Surface Pressure Coefficients**

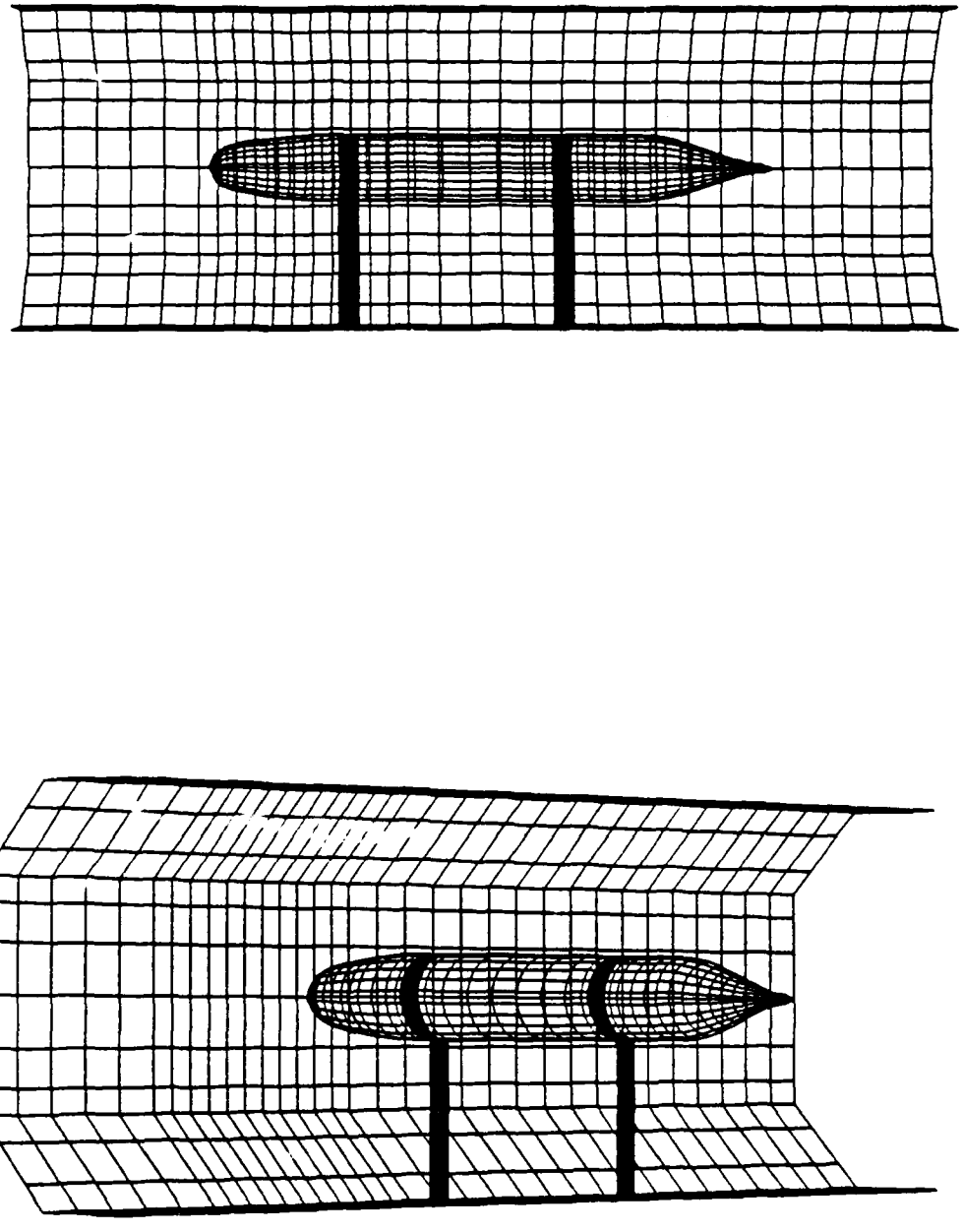

Figure 4 - Grid Representation Of Axisymmetric Hull With Struts Inside The AFF Wind Tunnel

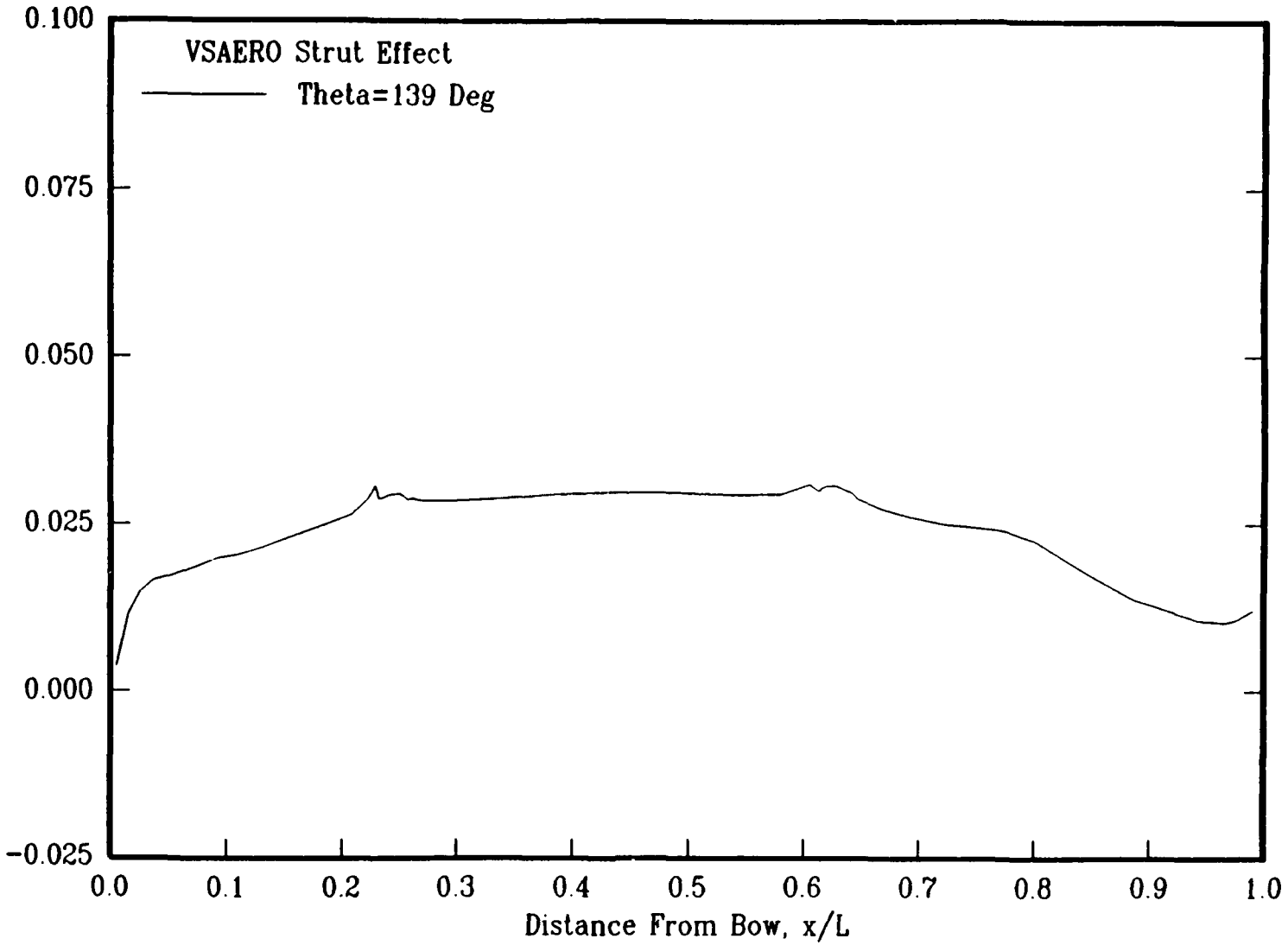

Figure 5-a - Effects Of Tunnel Blockage And Two Supporting Struts On The Computed Inviscid Surface Velocity, At Theta = 139 Deg.

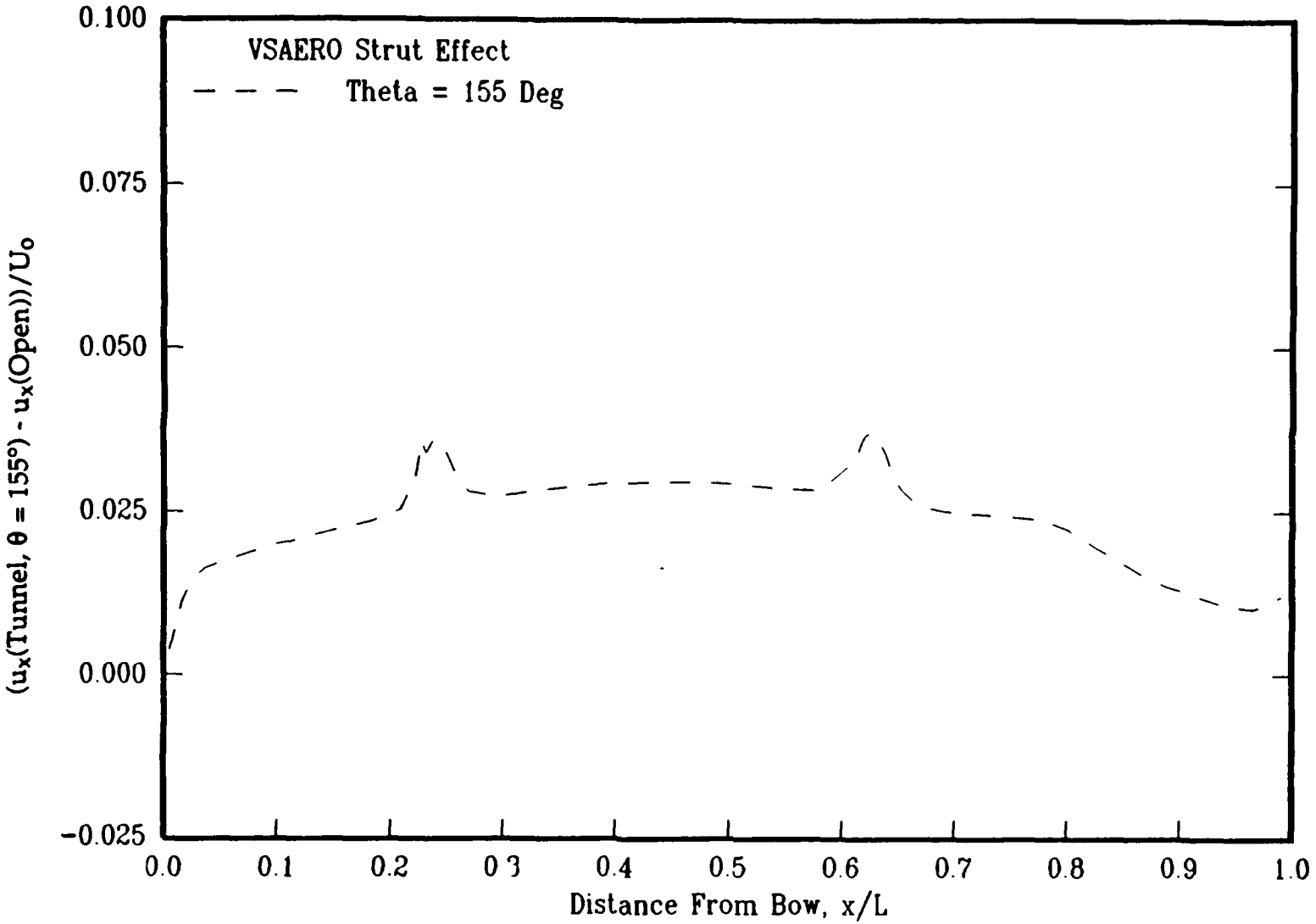

Figure 5-b - Effects Of Tunnel Blockage And Two Supporting Struts On The Computed Inviscid Surface Velocity, At Theta = 155 Deg.

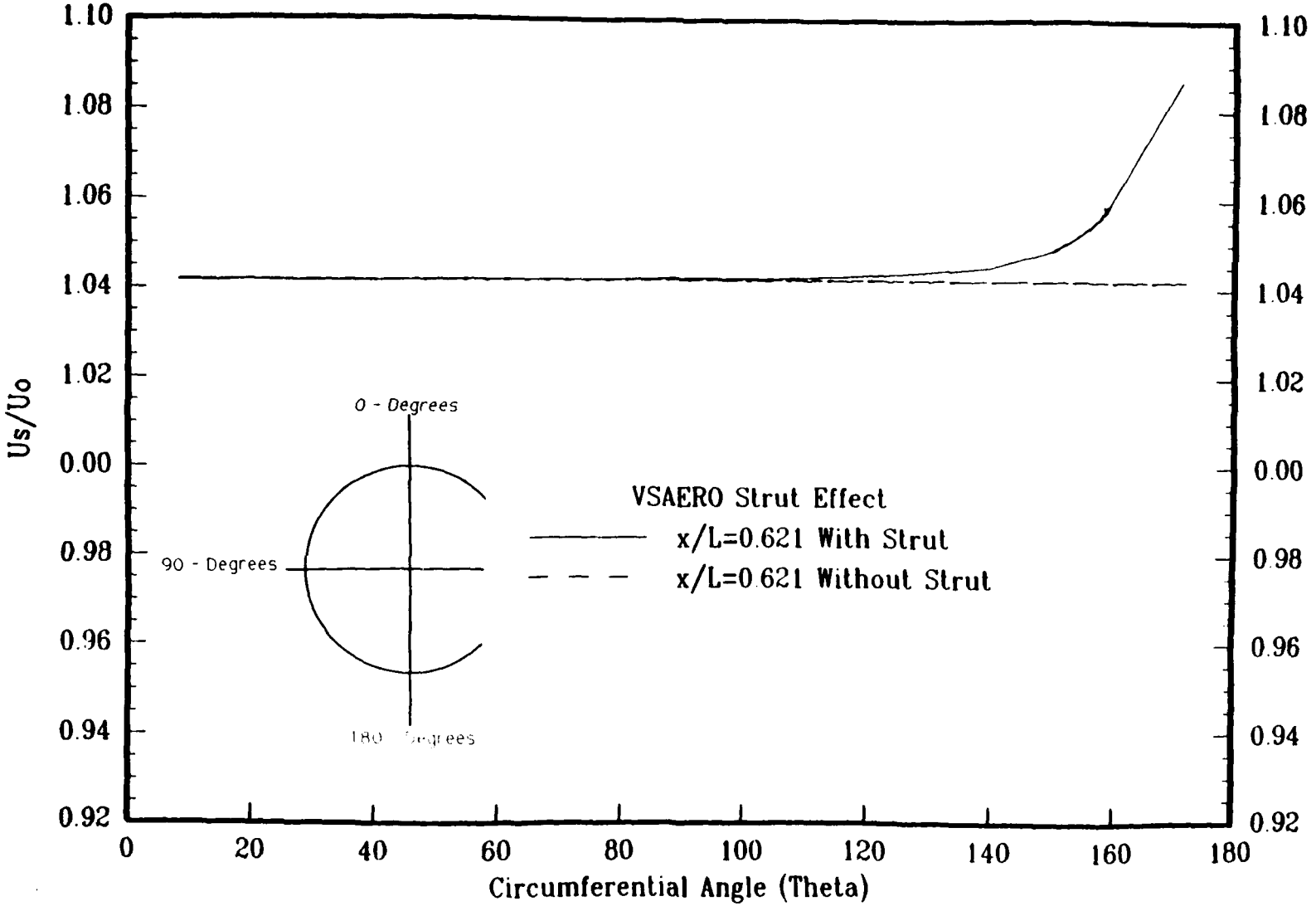

Figure 5-c - The Effect Of Struts On The Circumferentical Distribution Of Surface Potential Flow Velocities

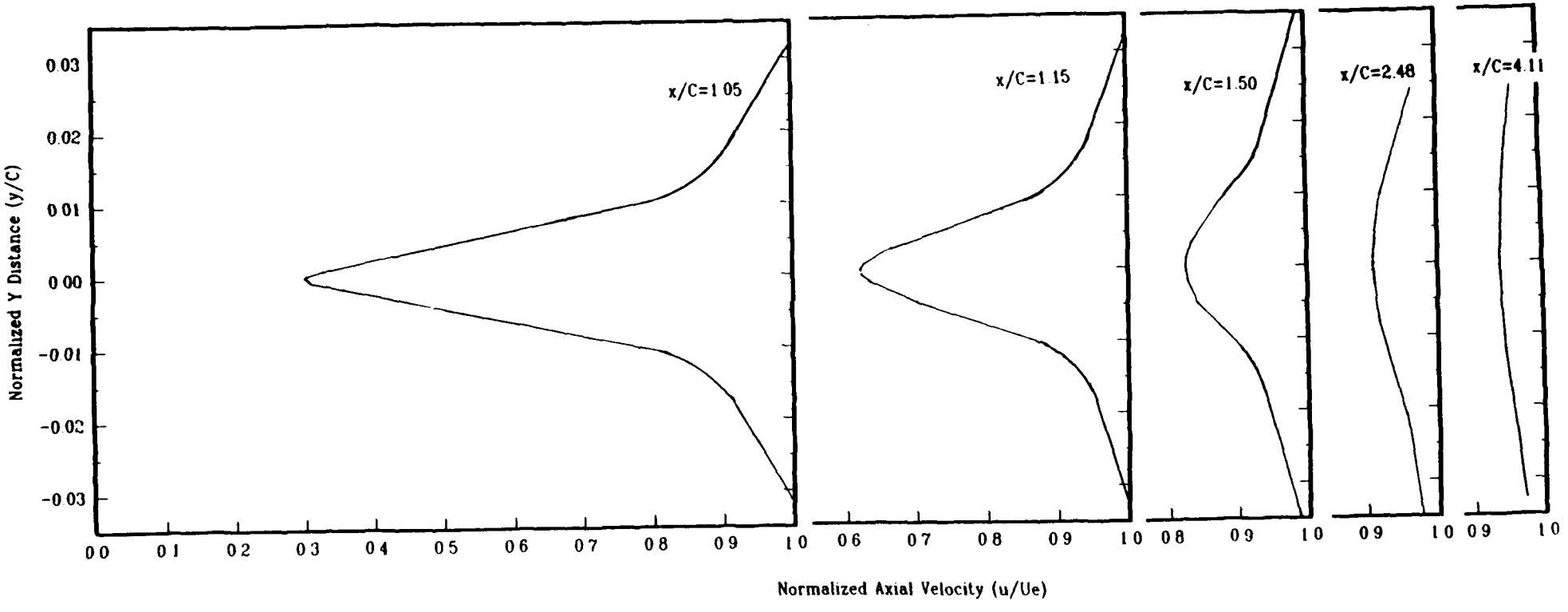

Figure 6 - The Strut Wakes Estimated By Two Dimensional Approximation

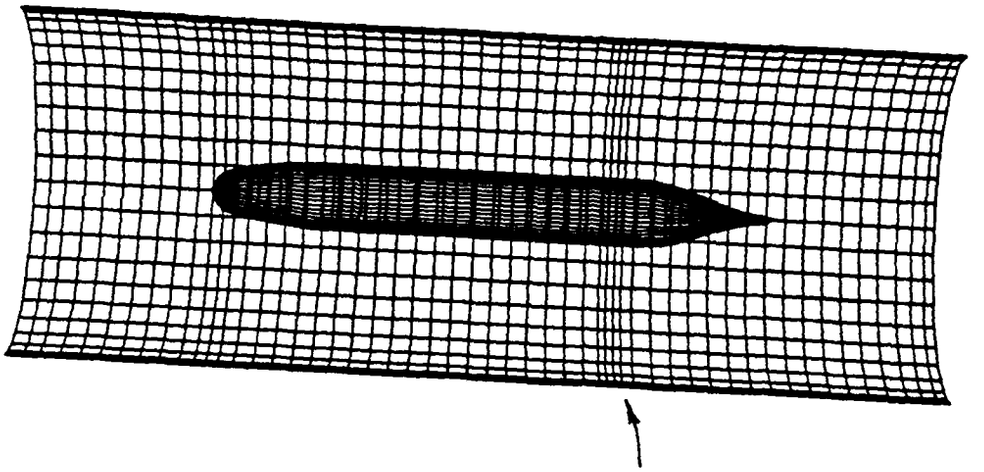

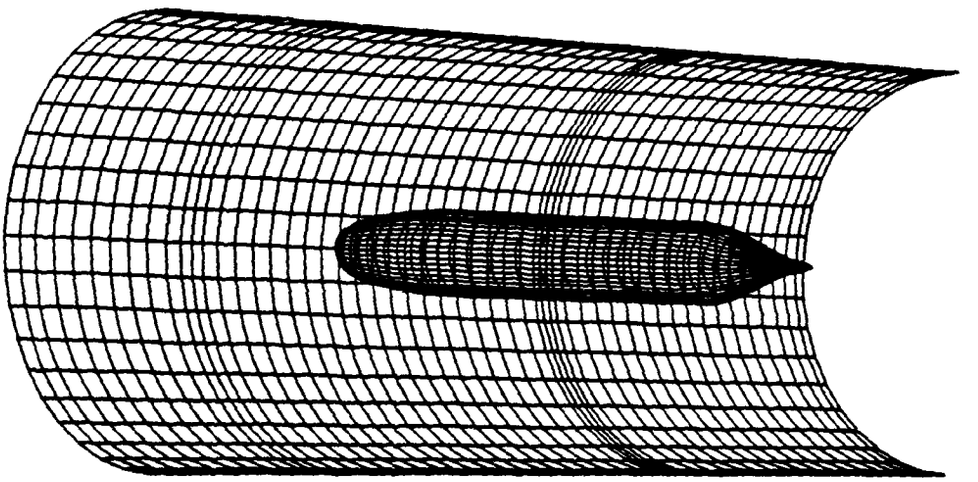

Figure 7 - **Grid Representation Of Axisymmetric Hull In A Circular Tunnel**

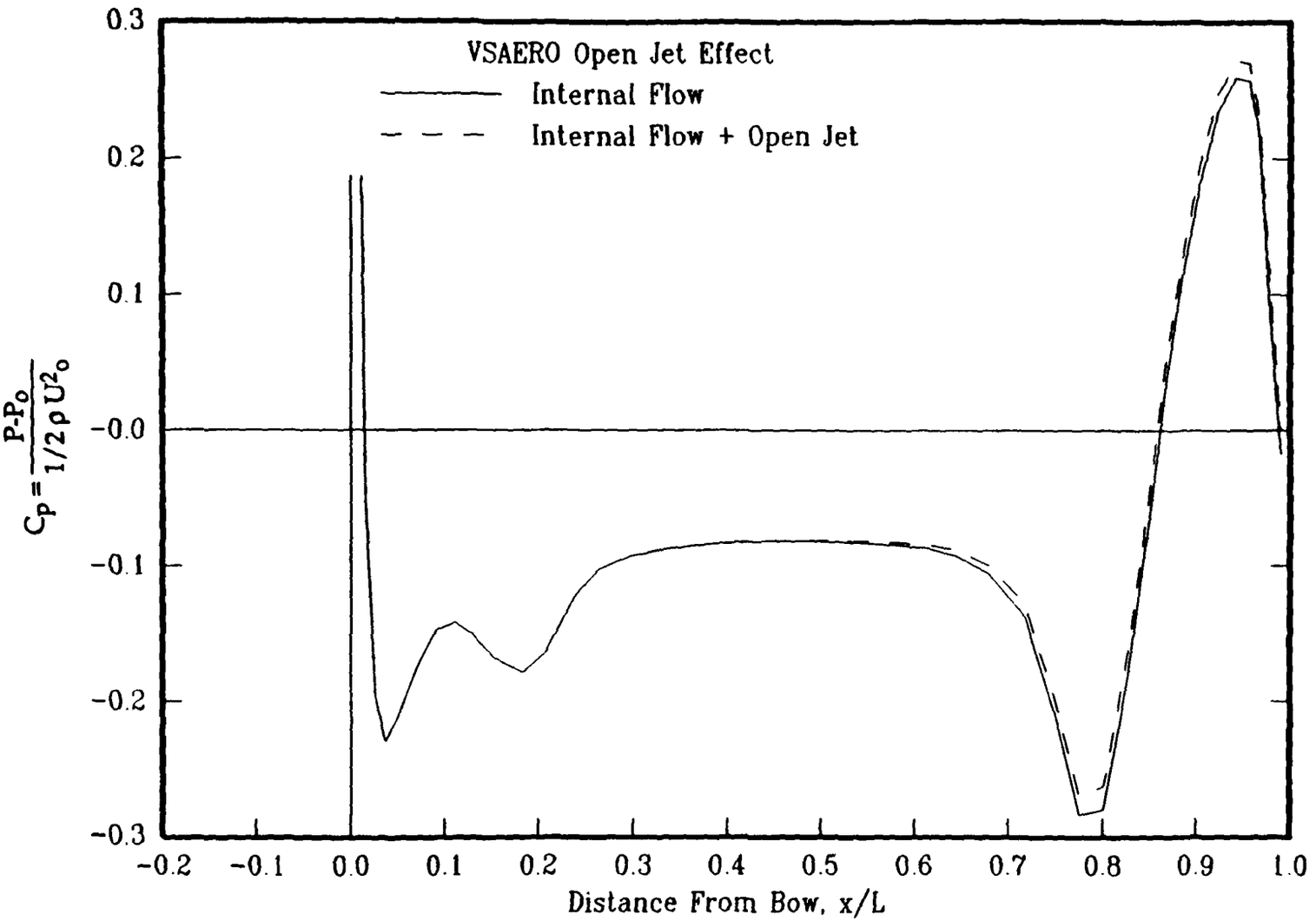

Figure 8 - Effect Of Jet Region On Computed Surface Pressure Coefficients

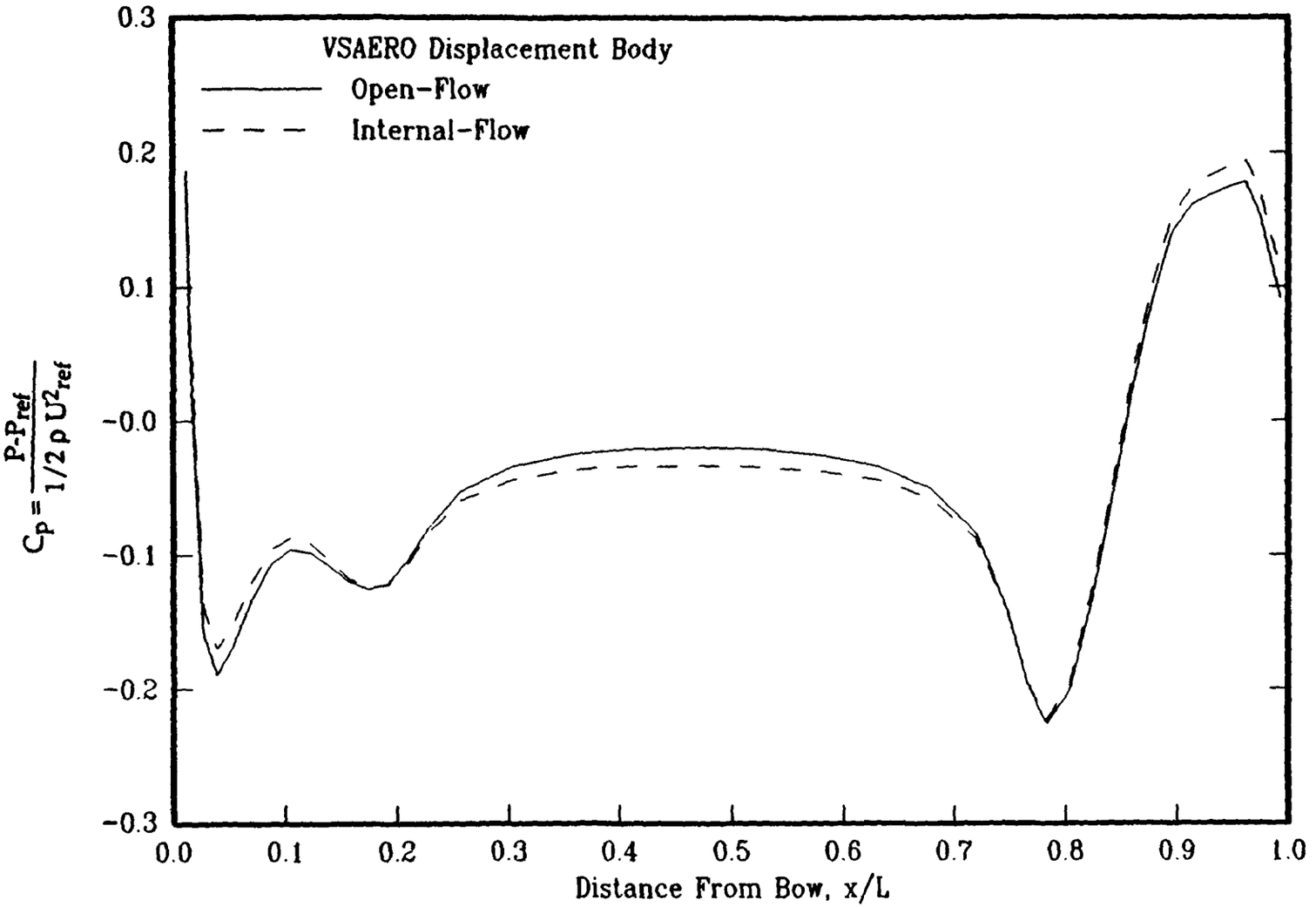

Figure 9 - Effect Of The Tunnel Blockage On The Computed Surface Pressure Coefficients Of A Displacement Model 5471 Normalized With U AT x/L = 0.85

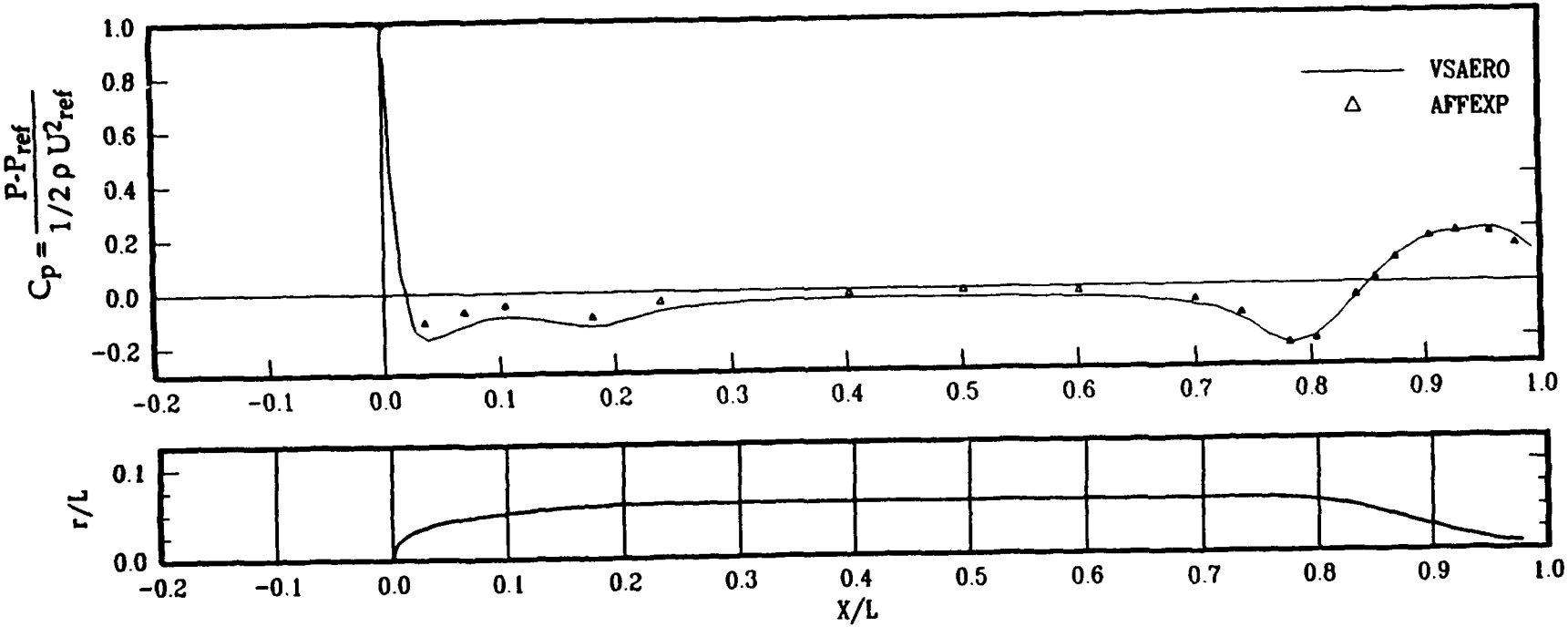

Figure 10 - Comparison Of The Measured And Computed Static Pressure Distribution Along The Model, Normalized With U At x/L = 0.85

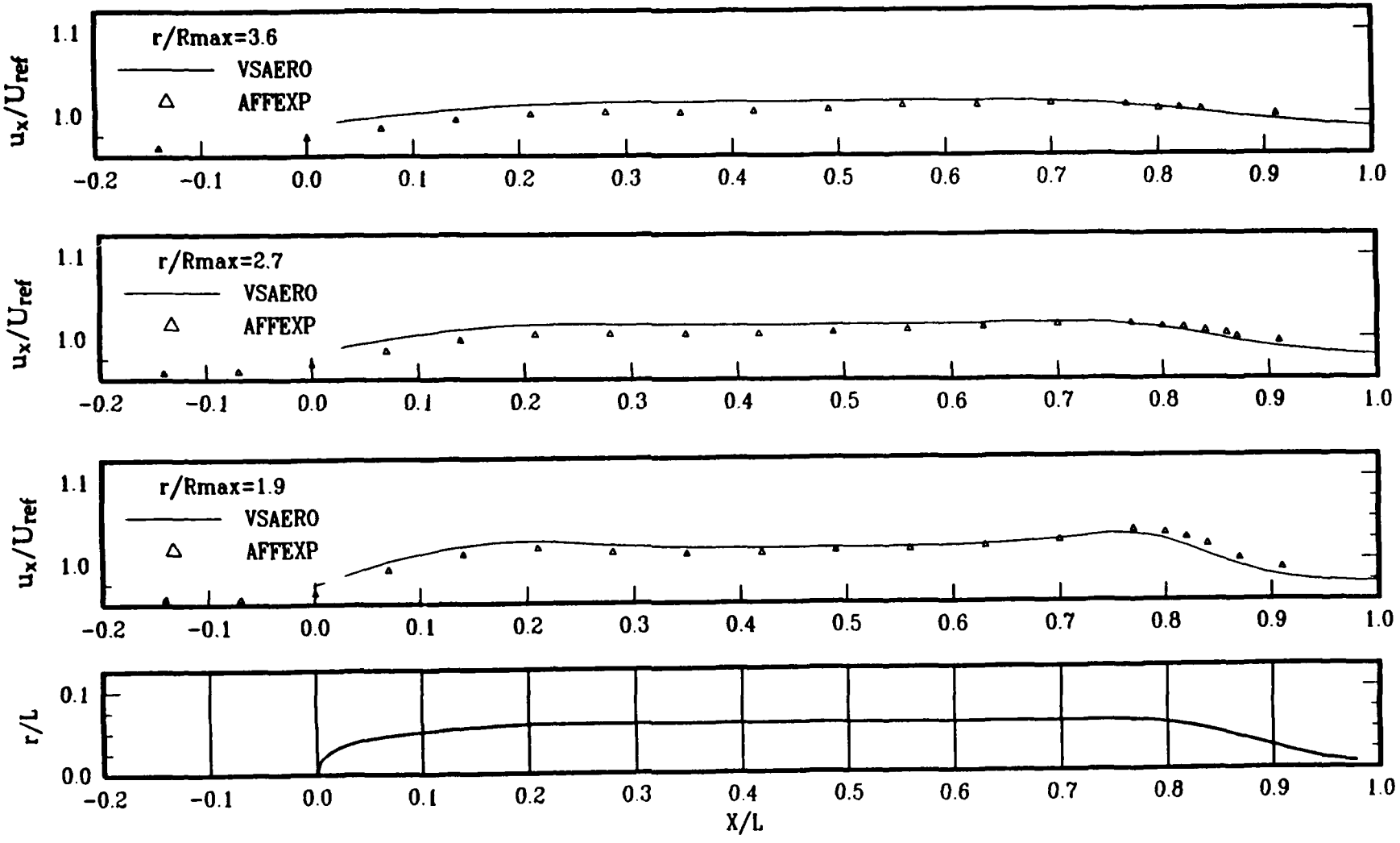

Figure 11 - Comparison Of Measured And Computed Velocities Along The Tunnel Axis Normalized With U At x/L = 0.85

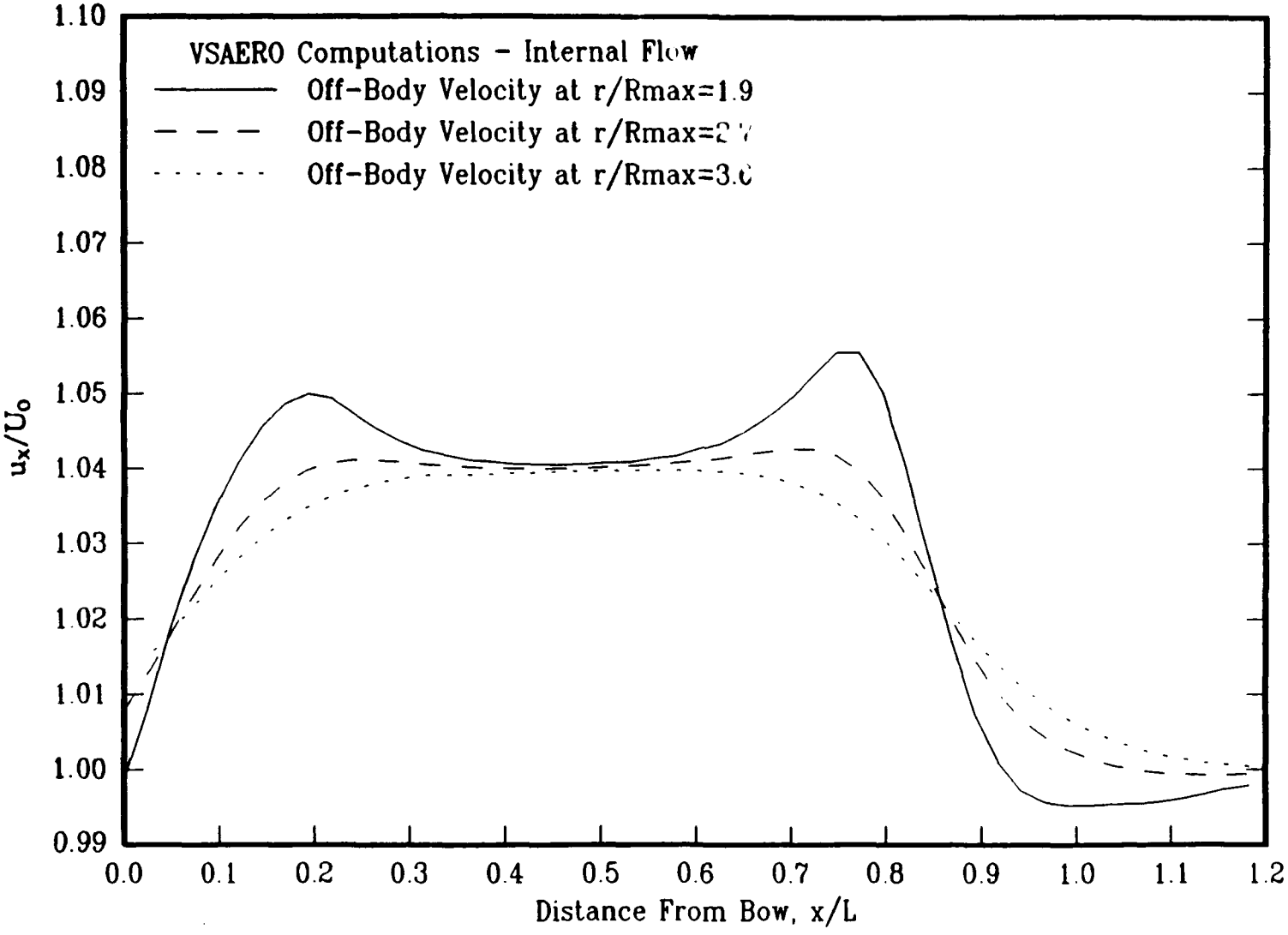

Figure 12-a - Computed Off-Body Velocities Inside The Tunnel -Internal Flow

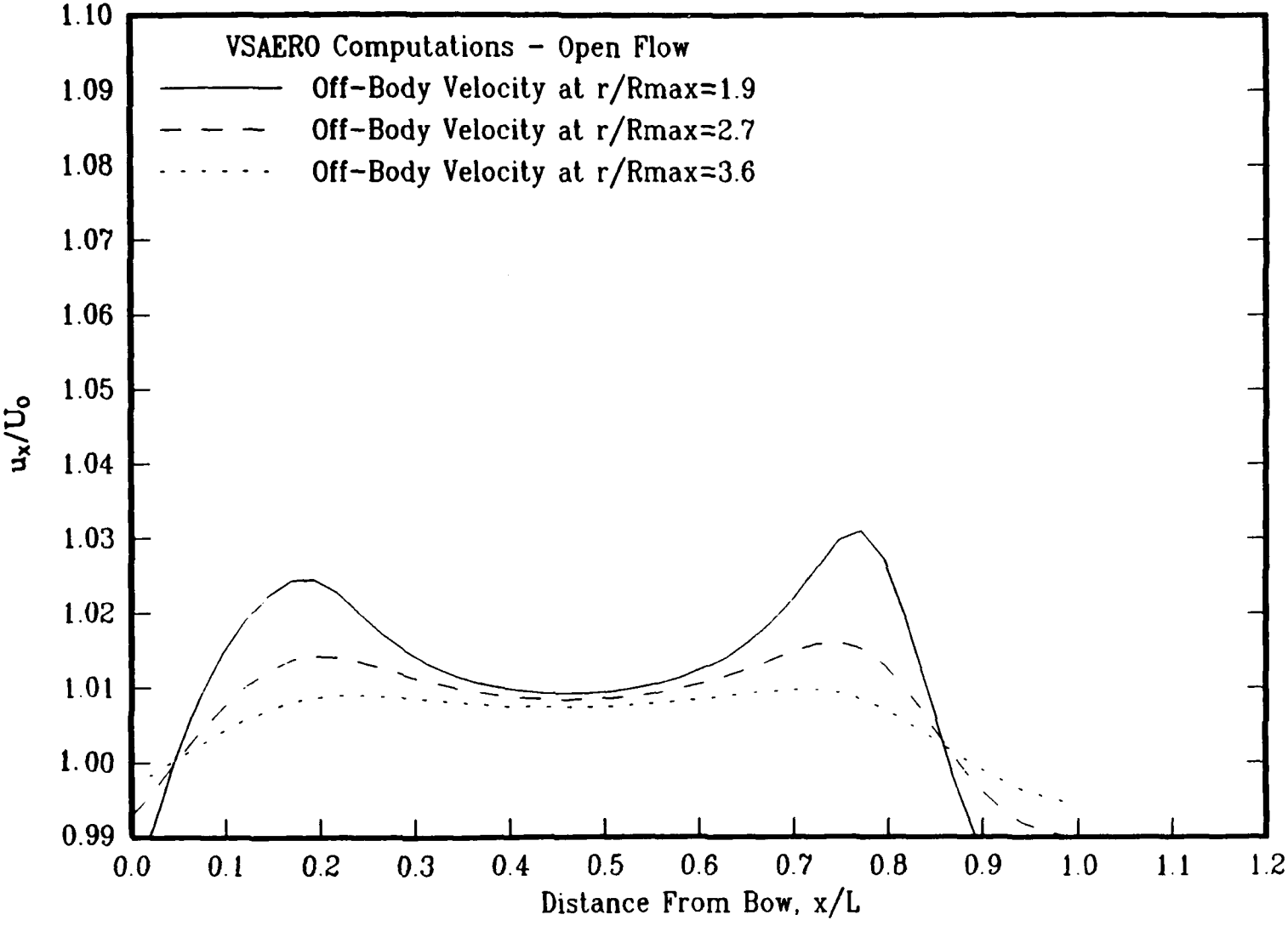

Figure 12-b - Computed Off-Body Velocities - Open Flow

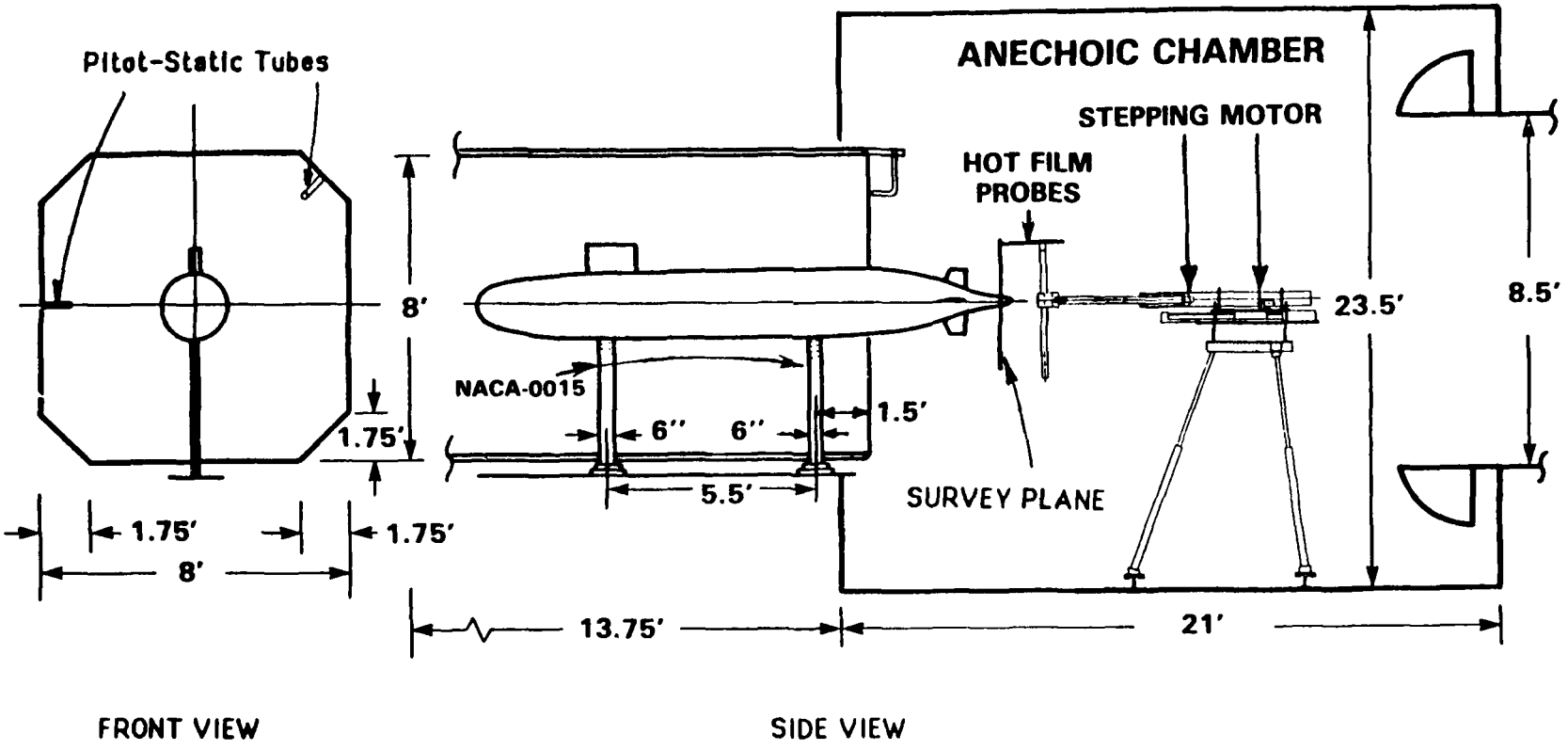

Figure 13 - Model Setup Inside The AFF Wind Tunnel

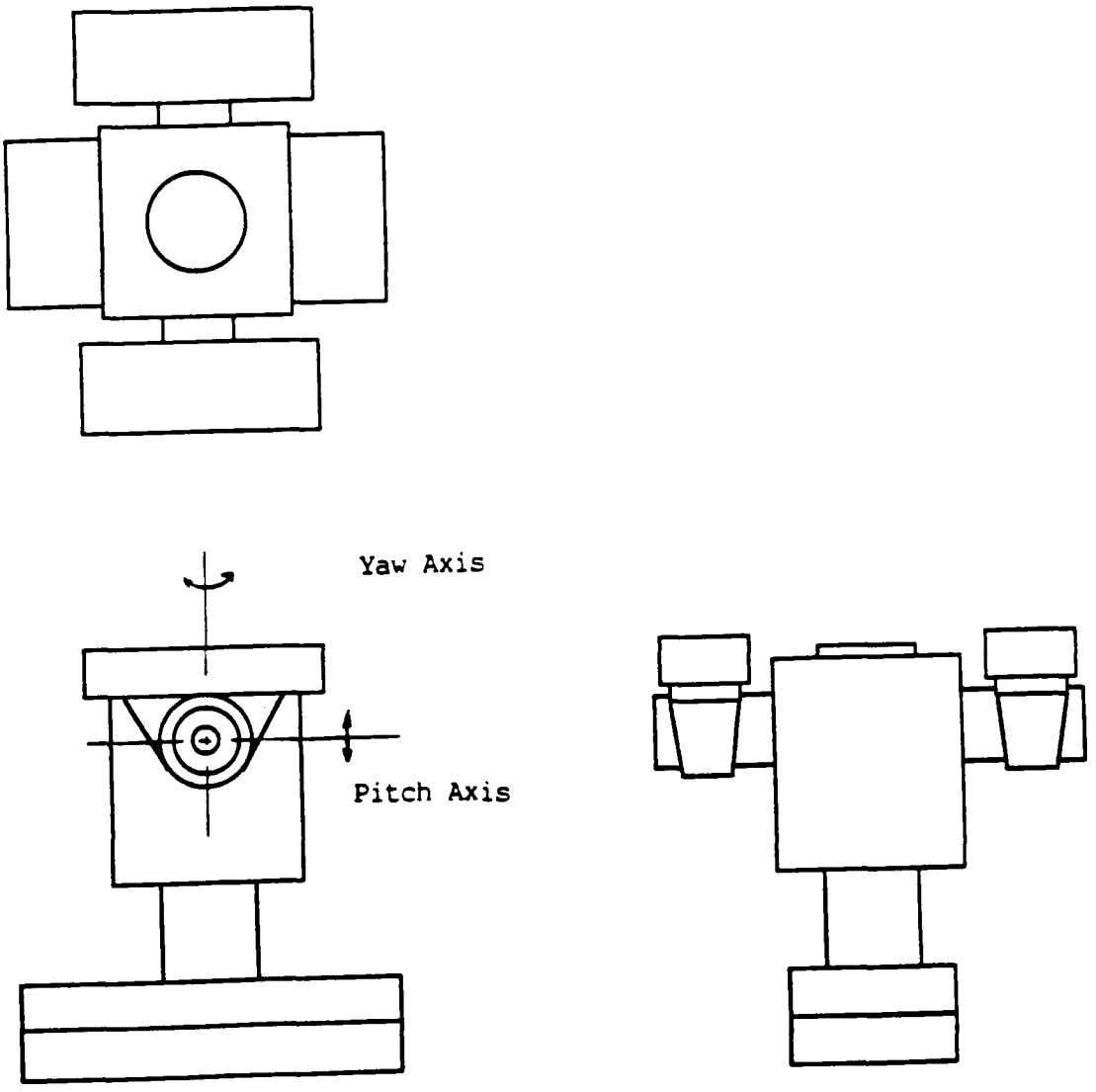

Figure 14 - Gimbal Assembly

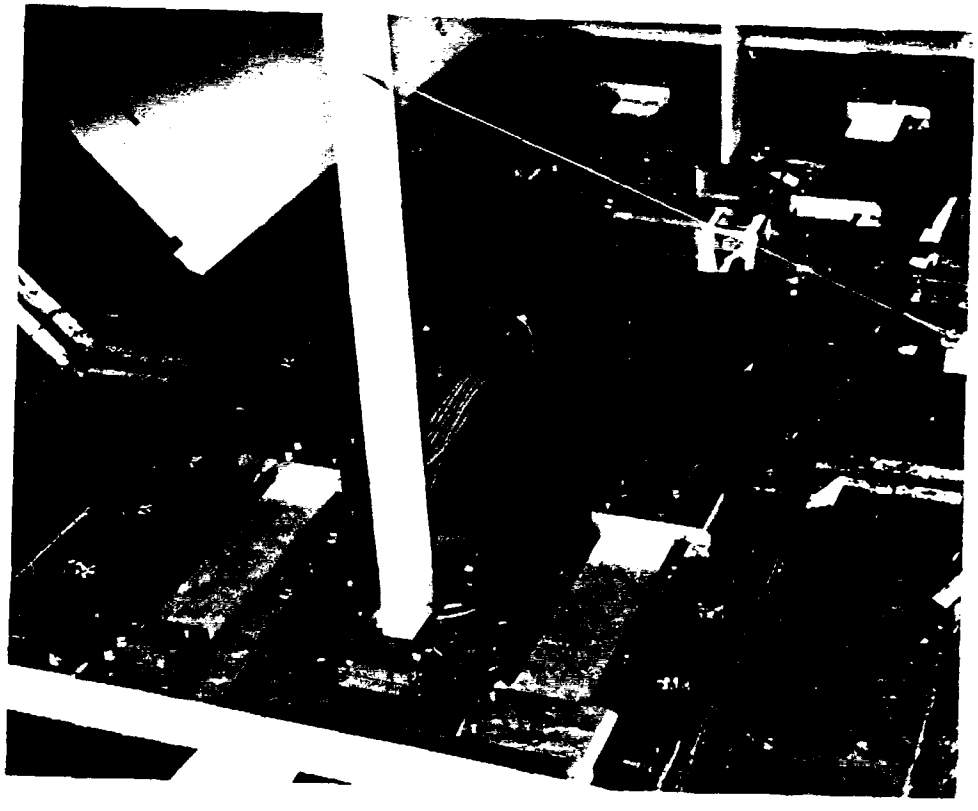

Figure 15 - Strut Base Design

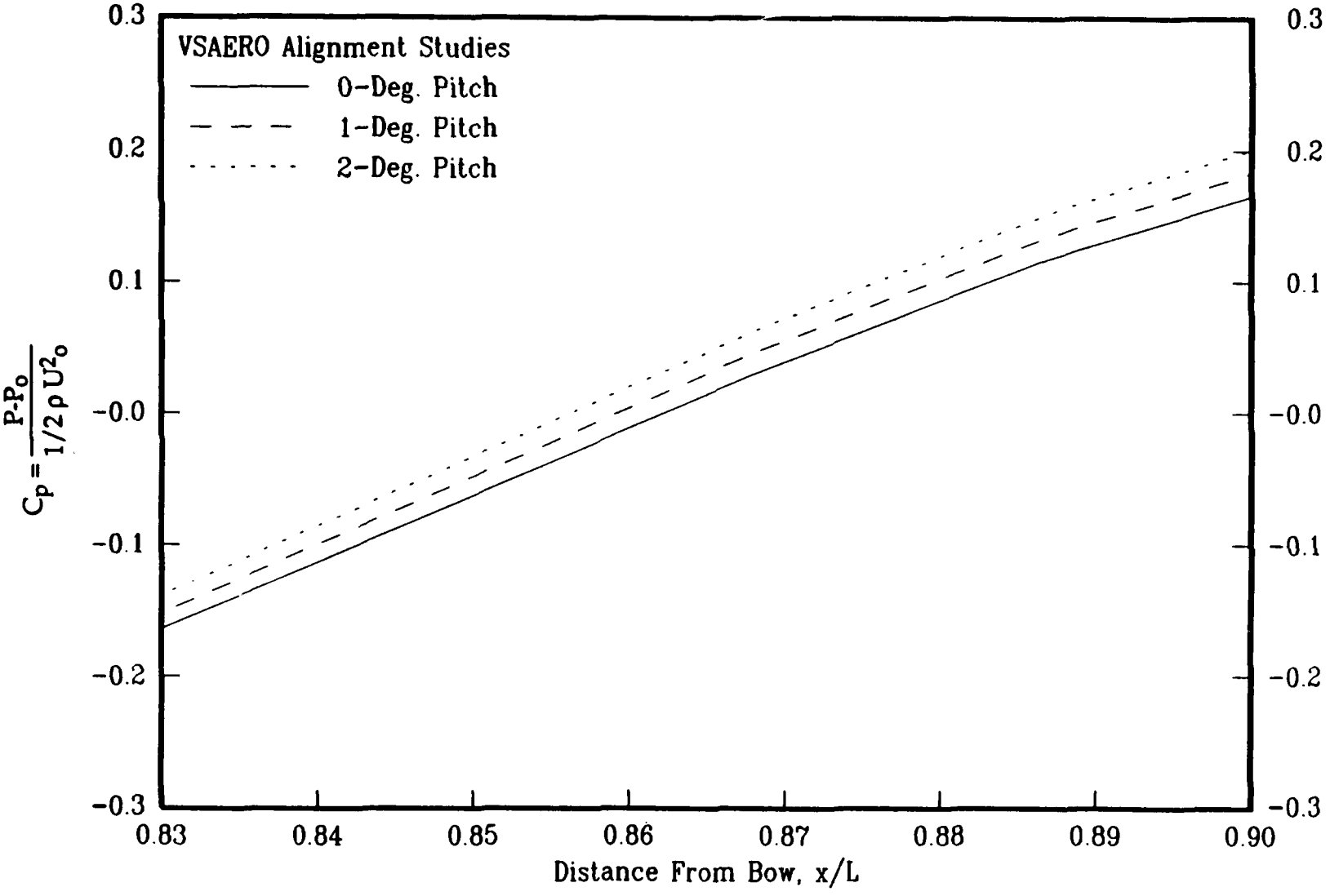

Figure 16 - Effect Of Model Alignment On Computed Surface Pressure Coefficients Along The Top Meridian Line. Theta = 0 Degree

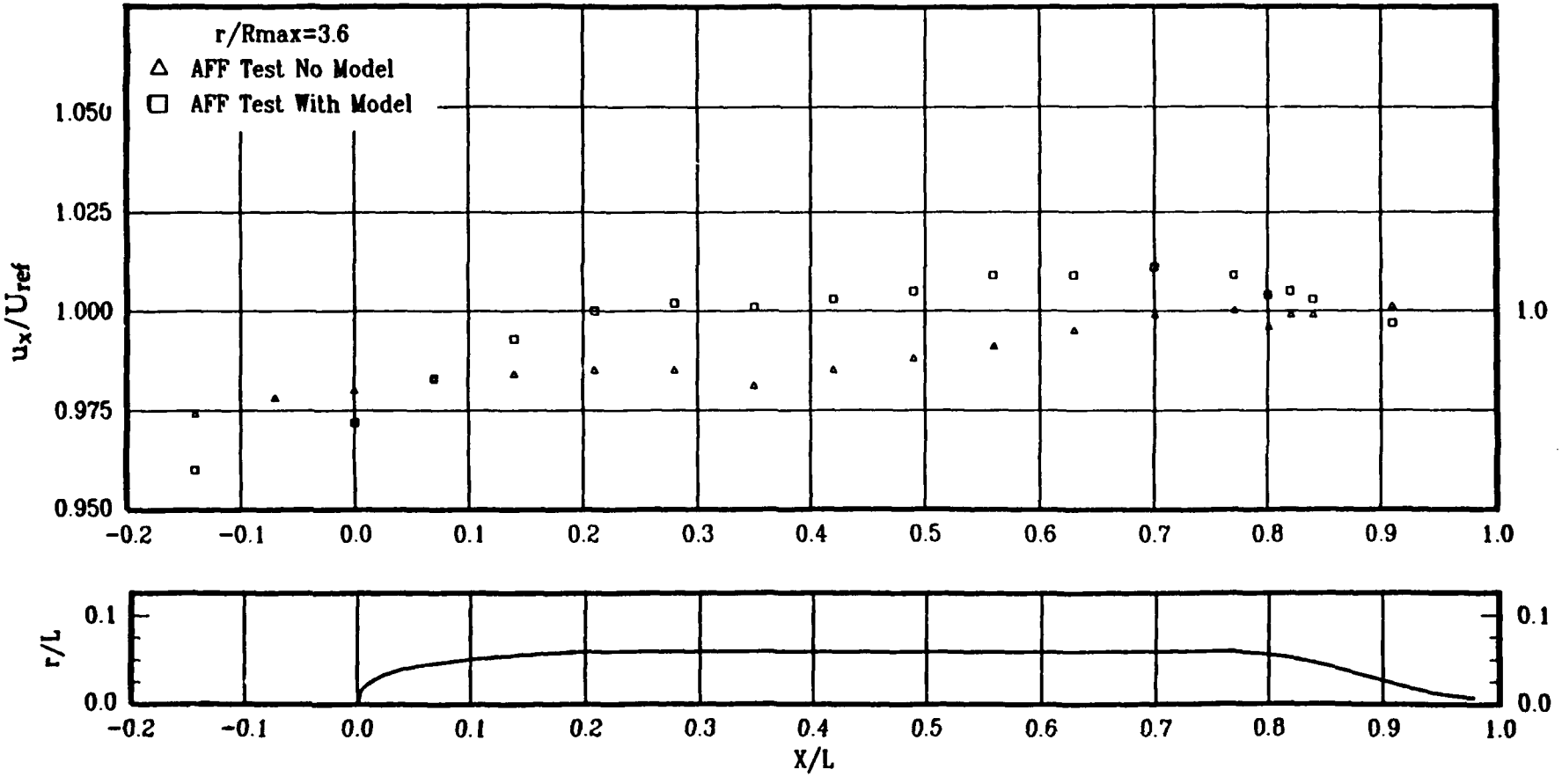

Figure 17 - Tunnel Velocity Survey Along The Ceiling With/Without Model Normalized With U At x/L = 0.85

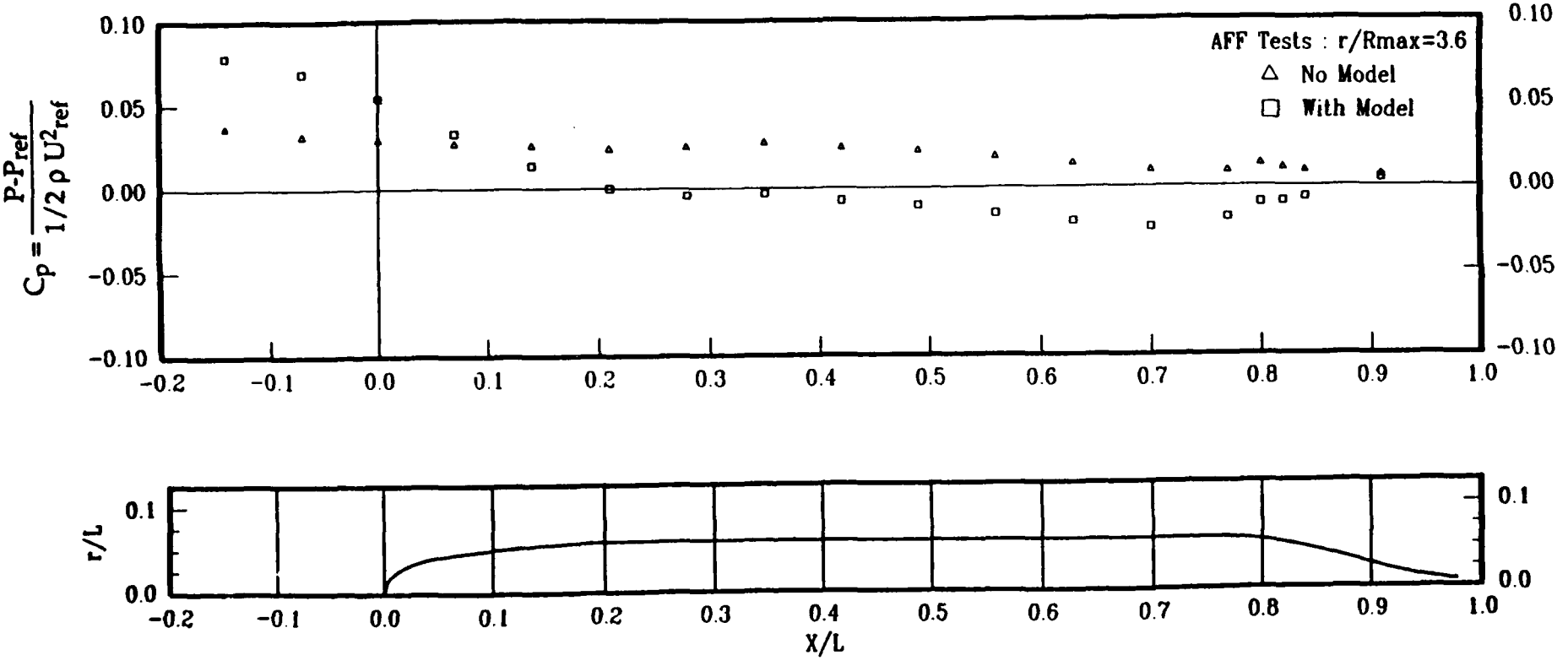

Figure 18 - Tunnel Static Pressure Survey Along The Ceiling With/Without Model

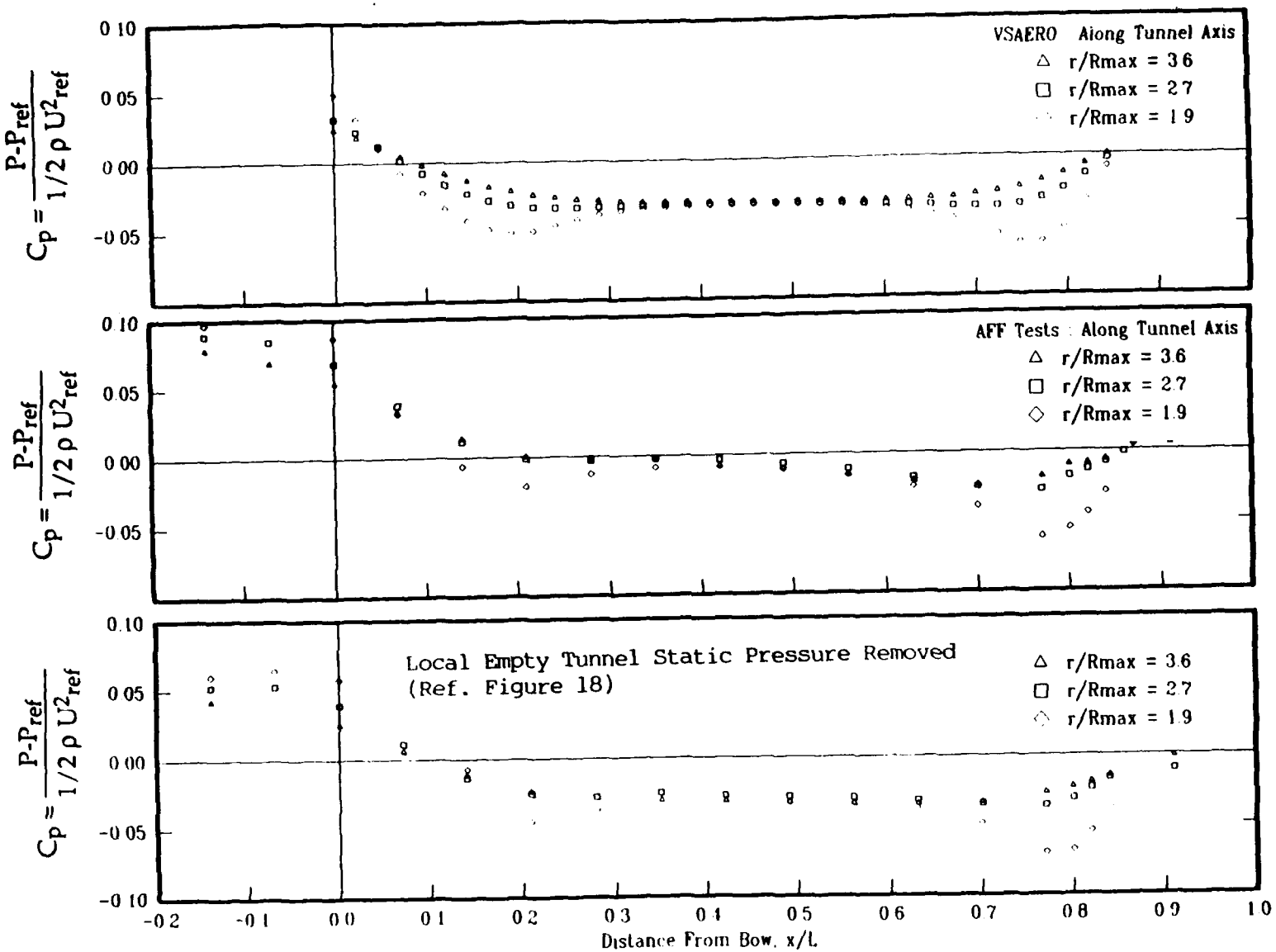

Figure 19 - Tunnel Static Pressure Computations And Measurements Along The Ceiling Centerline

TABLE 1 – MEASURED MODEL RADUIS OFFSETS

Distance from nose	Horizontal Centerline		Vertical Centerline		45°		45°		Seam		σ	Mean Radius (as built)	Designed Radius
	Port	Stbd	Bottom	Top	Port Upper	Stbd Lower	Port Lower	Stbd Upper	Port	Stbd			
1.2	3.32	3.47	3.42	3.60	3.34	3.50	3.44	3.54	3.35	3.61	0.099	3.459	3.406
2.4	4.50	4.60	4.56	4.64	4.56	4.60	4.54	4.65	4.50	4.64	0.053	4.579	4.569
3.6	5.30	5.37	5.36	5.43	5.33	5.36	5.36	5.44	5.27	5.42	0.052	5.364	5.362
4.8	5.89	5.93	5.92	6.00	5.93	5.94	5.92	6.00	5.86	5.96	0.042	5.935	5.935
6	6.34	6.38	6.36	6.40	6.36	6.38	6.36	6.42	6.31	6.41	0.032	6.372	6.393
9	7.15	7.18	7.20	7.21	7.18	7.18	7.16	7.22	7.12	7.22	0.031	7.182	7.212
12	7.70	7.74	7.76	7.78	7.73	7.74	7.74	7.77	7.67	7.78	0.033	7.741	7.780
18	8.57	8.61	8.62	8.63	8.59	8.63	8.61	8.64	8.55	8.65	0.030	8.610	8.624
24	9.24	9.27	9.32	9.29	9.27	9.30	9.29	9.29	9.22	9.30	0.028	9.278	9.293
31	9.78	9.80	9.82	9.80	9.80	9.80	9.80	9.80	9.78	9.82	0.013	9.800	9.825
41	9.97	9.97	---	9.98	10.00	10.00	9.97	9.96	9.94	9.99	0.018	9.996	10.000
86	10.00	9.99	10.00	10.00	9.99	10.00	10.00	9.98	10.00	10.00	0.070	9.996	10.000
127	10.03	9.93	10.00	9.96	10.00	10.00	10.01	9.90	10.05	9.95	0.044	9.983	10.000
134	9.83	9.70	9.80	9.73	9.80	9.75	9.82	9.69	9.84	9.72	0.053	9.768	9.796
144	7.87	7.75	7.85	7.80	7.86	7.80	7.88	7.74	7.88	7.75	0.054	7.818	7.856
155	4.24	4.06	4.18	4.12	4.21	4.10	4.22	4.09	4.23	4.05	0.070	4.150	4.174

Anechoic Flow Facility Model No. 5471 (units in inches)

σ = standard deviation = $\sqrt{\frac{\sum_{i=1}^{n} (x_i - \bar{x})^2}{n-1}}$

TABLE 1 (CONTINUED) – MEASURED MODEL RADUIS OFFSETS

Distance from nose	Horizontal		Vertical		45° Port Upper	45° Stbd Lower	45° Port Lower	45° Stbd Upper	Seam Port	Seam Stbd	σ	Mean Radius (as built)	Designed Radius
	Port	Stbd	Bottom	Top									
1.2	3.40	3.94	3.51	3.41	3.37	3.53	3.40	3.46	3.43	3.57	0.062	3.452	3.406
2.4	4.55	4.58	4.66	4.58	4.56	4.72	4.55	4.64	4.51	4.65	0.061	4.600	4.569
3.6	5.33	5.38	5.42	5.43	5.38	5.46	5.35	5.40	5.30	5.38	0.045	5.383	5.362
4.8	5.90	5.92	5.96	5.92	5.92	5.99	5.90	5.96	5.88	5.95	0.032	5.930	5.935
6	6.35	6.37	6.41	6.38	6.40	6.42	6.34	6.39	6.32	6.38	0.030	6.376	6.393
9	7.15	7.20	7.22	7.20	7.18	7.22	7.16	7.19	7.12	7.18	0.030	7.182	7.212
12	7.72	7.74	7.78	7.78	7.75	7.80	7.72	7.75	7.68	7.75	0.033	7.747	7.780
18	8.58	8.63	8.64	8.64	8.61	8.66	8.60	8.63	8.53	8.41	0.070	8.593	8.624
24	9.24	9.30	9.30	9.31	9.28	9.32	9.27	9.29	9.24	9.27	0.026	9.282	9.293
31	9.78	9.83	9.82	9.82	9.80	9.84	9.80	9.80	9.78	9.82	0.019	9.809	9.825
41	9.98	10.00	---	10.00	9.99	10.01	10.02	10.00	9.98	9.98	0.013	9.996	10.000
86	10.00	10.00	10.02	10.02	10.00	10.02	10.00	10.00	10.00	10.00	0.009	10.006	10.000
127	10.03	9.96	10.03	10.00	9.98	10.05	10.02	9.95	10.00	9.94	0.036	9.996	10.000
134	9.84	9.73	9.81	9.80	9.78	9.83	9.82	9.71	9.82	9.73	0.045	9.787	9.796
144	7.87	7.76	7.87	7.84	7.84	7.87	7.84	7.76	7.86	7.79	0.042	7.830	7.856
155	4.21	4.15	4.18	4.17	4.18	4.21	4.25	4.14	4.22	4.17	0.032	4.188	4.174

Anechoic Flow Facility Model No. 5470 (units in inches)

σ = standard deviation = $\sqrt{\frac{\sum_{i=1}^{n} (x_i - \bar{x})^2}{n-1}}$

APPENDIX A

SAMPLE INPUTS FOR

VSAERO PROGRAM

```
DARPA2 SUBOFF - BARE HULL W/ STRUT IN CHAMBER
  0    5    0    0
  0    0    0
  1 3000
  0    0    0
0.0       0.0
0.0
2.0       100.0     2.0
  2    0    0    0
  1                    1.0
  2                   -1.0
0.0       0.0       0.0       1.0       0.0
  2    0    1    1     *INLET ; X=-5.
    0.0       0.0       0.0       12.0      0.0       0.0    4
  -5.00       0.0       4.00
  -5.00       0.0       3.50
  -5.00       0.0       2.75
  -5.00       0.0       2.25
  -5.00       0.0       1.75
  -5.00       0.0       1.00
  -5.00       0.0       0.00
  -5.00       0.0      -1.00
  -5.00       0.0      -1.75
  -5.00       0.0      -2.25
  -5.00       0.0      -2.75
  -5.00       0.0      -3.50
  -5.00       0.0      -4.00
                                3
    0.0       0.0       0.0       12.0      0.0       0.0    4    3    5    3
  -5.00       2.25      4.00
  -5.00       2.75      3.50
  -5.00       3.50      2.75
  -5.00       4.00      2.25
  -5.00       4.00      1.75
  -5.00       4.00      1.00
  -5.00       4.00      0.00
  -5.00       4.00     -1.00
  -5.00       4.00     -1.75
  -5.00       4.00     -2.25
  -5.00       3.50     -2.75
  -5.00       2.75     -3.50
  -5.00       2.25     -4.00
                                3
  2    0    1    1     *OUTLET ; X=19.
    0.0       0.0       0.0       12.0      0.0       0.0    4
  19.00       2.25      4.00
  19.00       2.75      3.50
  19.00       3.50      2.75
  19.00       4.00      2.25
  19.00       4.00      1.75
  19.00       4.00      1.00
  19.00       4.00      0.00
  19.00       4.00     -1.00
  19.00       4.00     -1.75
  19.00       4.00     -2.25
  19.00       3.50     -2.75
  19.00       2.75     -3.50
  19.00       2.25     -4.00
                                3
    0.0       0.0       0.0       12.0      0.0       0.0    4    3    5    3
  19.00       0.0       4.00
  19.00       0.0       3.50
  19.00       0.0       2.75
```

```
    19.00        0.0       2.25
    19.00        0.0       1.75
    19.00        0.0       1.00
    19.00        0.0       0.00
    19.00        0.0      -1.00
    19.00        0.0      -1.75
    19.00        0.0      -2.25
    19.00        0.0      -2.75
    19.00        0.0      -3.50
    19.00        0.0      -4.00
                                                    3
   2    0    1    1      *BOR - FWD
  0.0     0.0       0.0        12.0000   0.0       0.0          2   -3   11    3
   0.00000   0.00000
   0.15000   0.33803
   0.30000   0.44599
   0.45000   0.51473
   0.60000   0.56368
   0.88000   0.62732
   1.16000   0.67313
   1.44000   0.71105
   1.72000   0.74468
   2.00000   0.77440
   2.41667   0.80892
   2.83333   0.82831
   3.11000   0.83281
   3.25000   0.83333
                                                    3
 180.       0.0
    2    0    1    1      *BOR - FWD STRUT
  0.0     0.0       0.0        12.0000   0.0       0.0          2   -2   10    3
   3.25000   0.83333
   3.26250   0.83333
   3.27500   0.83333
   3.30000   0.83333
   3.32500   0.83333
   3.35000   0.83333
   3.40000   0.83333
   3.45000   0.83333
   3.50000   0.83333
   3.55000   0.83333
   3.60000   0.83333
   3.65000   0.83333
   3.70000   0.83333
   3.72500   0.83333
   3.75000   0.83333
                                                    3
 163.6364  0.0
  0.0     0.0       0.0        12.0000   0.0       0.0          4
   3.25000   0.23478 -0.79958
   3.26250   0.23478 -0.79958
   3.27500   0.23478 -0.79958
   3.30000   0.23478 -0.79958
   3.32500   0.23478 -0.79958
   3.35000   0.23478 -0.79958
   3.40000   0.23478 -0.79958
   3.45000   0.23478 -0.79958
   3.50000   0.23478 -0.79958
   3.55000   0.23478 -0.79958
   3.60000   0.23478 -0.79958
   3.65000   0.23478 -0.79958
   3.70000   0.23478 -0.79958
   3.72500   0.23478 -0.79958
```

```
   3.75000    0.23478 -0.79958
                                        3
  0.0      0.0        0.0        12.0000    0.0        0.0          4    3    0    3
   3.25000    0.00000  -0.83333
   3.26250    0.00817  -0.83329
   3.27500    0.01111  -0.83326
   3.30000    0.01463  -0.83320
   3.32500    0.01671  -0.83316
   3.35000    0.01793  -0.83314
   3.40000    0.01876  -0.83312
   3.45000    0.01814  -0.83313
   3.50000    0.01654  -0.83317
   3.55000    0.01426  -0.83321
   3.60000    0.01145  -0.83325
   3.65000    0.00820  -0.83329
   3.70000    0.00452  -0.83332
   3.72500    0.00252  -0.83333
   3.75000    0.00040  -0.83333
                                        3
    2    0    1    1      *BOR - MID
  0.0      0.0        0.0        12.0000    0.0        0.0          2   -3   11    3
   3.75000    0.83333
   3.95000    0.83333
   4.46429    0.83333
   5.17857    0.83333
   5.89286    0.83333
   6.60714    0.83333
   7.32143    0.83333
   8.03572    0.83333
   8.55000    0.83333
   8.75000    0.83333
                                        3
 180.       0.0
    2    0    1    1      *BOR - AFT STRUT
  0.0      0.0        0.0        12.0000    0.0        0.0          2   -2   10    3
   8.75000    0.83333
   8.76250    0.83333
   8.77500    0.83333
   8.80000    0.83333
   8.82500    0.83333
   8.85000    0.83333
   8.90000    0.83333
   8.95000    0.83333
   9.00000    0.83333
   9.05000    0.83333
   9.10000    0.83333
   9.15000    0.83333
   9.20000    0.83333
   9.22500    0.83333
   9.25000    0.83333
                                        3
 163.6364   0.0
  0.0      0.0        0.0        12.0000    0.0        0.0          4
   8.75000    0.23478 -0.79958
   8.76250    0.23478 -0.79958
   8.77500    0.23478 -0.79958
   8.80000    0.23478 -0.79958
   8.82500    0.23478 -0.79958
   8.85000    0.23478 -0.79958
   8.90000    0.23478 -0.79958
   8.95000    0.23478 -0.79958
   9.00000    0.23478 -0.79958
   9.05000    0.23478 -0.79958
```

```
 9.10000   0.23478 -0.79958
 9.15000   0.23478 -0.79958
 9.20000   0.23478 -0.79958
 9.22500   0.23478 -0.79958
 9.25000   0.23478 -0.79958
                                        3
0.0     0.0       0.0       12.0000   0.0       0.0          4   3   0   3
 8.75000   0.00000  -0.83333
 8.76250   0.00817  -0.83329
 8.77500   0.01111  -0.83326
 8.80000   0.01463  -0.83320
 8.82500   0.01671  -0.83316
 8.85000   0.01793  -0.83314
 8.90000   0.01876  -0.83312
 8.95000   0.01814  -0.83313
 9.00000   0.01654  -0.83317
 9.05000   0.01426  -0.83321
 9.10000   0.01145  -0.83325
 9.15000   0.00820  -0.83329
 9.20000   0.00452  -0.83332
 9.22500   0.00252  -0.83333
 9.25000   0.00040  -0.83333
                                        3
  2    0    1    1     *BOR - AFT
0.0     0.0       0.0       12.0000   0.0       0.0          2  -3  11   3
 9.25000   0.83333
 9.40000   0.83333
 9.66667   0.83333
10.08333   0.83333
10.50000   0.83333
10.87500   0.83159
11.25000   0.80819
11.62500   0.74853
12.00000   0.65467
12.26667   0.57222
12.53333   0.48181
12.80000   0.38842
13.06667   0.29726
13.33333   0.21382
13.60000   0.14482
13.73833   0.11835
13.87667   0.10182
14.01500   0.09727
14.29167   0.00000
                                      3
180.      0.0
   1    0    1    1     *STRUT - FWD
 0.0     0.0       0.0       12.0000   0.0       0.0          4
 3.25000   0.00000  -0.83333
 3.26250   0.00817  -0.83329
 3.27500   0.01111  -0.83326
 3.30000   0.01463  -0.83320
 3.32500   0.01671  -0.83316
 3.35000   0.01793  -0.83314
 3.40000   0.01876  -0.83312
 3.45000   0.01814  -0.83313
 3.50000   0.01654  -0.83317
 3.55000   0.01426  -0.83321
 3.60000   0.01145  -0.83325
 3.65000   0.00820  -0.83329
 3.70000   0.00452  -0.83332
 3.72500   0.00252  -0.83333
 3.75000   0.00040  -0.83333
```

```
                                                    3
0.0      0.0        0.0          12.0000    0.0          0.0              4    3    8    2
 3.25000    0.00000   -4.00000
 3.26250    0.00817   -4.00000
 3.27500    0.01111   -4.00000
 3.30000    0.01463   -4.00000
 3.32500    0.01671   -4.00000
 3.35000    0.01793   -4.00000
 3.40000    0.01876   -4.00000
 3.45000    0.01814   -4.00000
 3.50000    0.01654   -4.00000
 3.55000    0.01426   -4.00000
 3.60000    0.01145   -4.00000
 3.65000    0.00820   -4.00000
 3.70000    0.00452   -4.00000
 3.72500    0.00252   -4.00000
 3.75000    0.00040   -4.00000
                                                    3
  1    0    1    1      *STRUT - AFT
0.0      0.0        0.0          12.0000    0.0          0.0              4
 8.75000    0.00000   -0.83333
 8.76250    0.00817   -0.83329
 8.77500    0.01111   -0.83326
 8.80000    0.01463   -0.83320
 8.82500    0.01671   -0.83316
 8.85000    0.01793   -0.83314
 8.90000    0.01876   -0.83312
 8.95000    0.01814   -0.83313
 9.00000    0.01654   -0.83317
 9.05000    0.01426   -0.83321
 9.10000    0.01145   -0.83325
 9.15000    0.00820   -0.83329
 9.20000    0.00452   -0.83332
 9.22500    0.00252   -0.83333
 9.25000    0.00040   -0.83333
                                                    3
0.0      0.0        0.0          12.0000    0.0          0.0              4    3    8    2
 8.75000    0.00000   -4.00000
 8.76250    0.00817   -4.00000
 8.77500    0.01111   -4.00000
 8.80000    0.01463   -4.00000
 8.82500    0.01671   -4.00000
 8.85000    0.01793   -4.00000
 8.90000    0.01876   -4.00000
 8.95000    0.01814   -4.00000
 9.00000    0.01654   -4.00000
 9.05000    0.01426   -4.00000
 9.10000    0.01145   -4.00000
 9.15000    0.00820   -4.00000
 9.20000    0.00452   -4.00000
 9.22500    0.00252   -4.00000
 9.25000    0.00040   -4.00000
                                                    3
  2    0    1    1      *CHAMBER
-60.00        0.0          0.0          12.0          0.0          0.0          1
  0.00        4.00
  0.75        4.00
  1.50        4.00
  2.25        4.00
  2.75        3.50
  3.50        2.75
  4.00        2.25
  4.00        1.75
```

```
  4.00      1.00
  4.00      0.00
  4.00     -1.00
  4.00     -1.75
  4.00     -2.25
  3.50     -2.75
  2.75     -3.50
  2.25     -4.00
  1.50     -4.00
  0.75     -4.00
  0.00     -4.00
                          3
 -6.00      0.0     0.0     12.0      0.0      0.0     1   2   5   3
  0.00      4.00
  0.75      4.00
  1.50      4.00
  2.25      4.00
  2.75      3.50
  3.50      2.75
  4.00      2.25
  4.00      1.75
  4.00      1.00
  4.00      0.00
  4.00     -1.00
  4.00     -1.75
  4.00     -2.25
  3.50     -2.75
  2.75     -3.50
  2.25     -4.00
  1.50     -4.00
  0.75     -4.00
  0.00     -4.00
                          3
 -6.00      0.0     0.0     12.0      0.0      0.0     1
  0.00      4.00
  0.75      4.00
  1.50      4.00
  2.25      4.00
  2.75      3.50
  3.50      2.75
  4.00      2.25
  4.00      1.75
  4.00      1.00
  4.00      0.00
  4.00     -1.00
  4.00     -1.75
  4.00     -2.25
  3.50     -2.75
  2.75     -3.50
  2.25     -4.00
  1.50     -4.00
  0.75     -4.00
  0.00     -4.00
                          3
 60.00      0.0     0.0     12.0      0.0      0.0     1   2   11  3
  0.00      4.00
  0.75      4.00
  1.50      4.00
  2.25      4.00
  2.75      3.50
  3.50      2.75
  4.00      2.25
  4.00      1.75
```

```
 4.00      1.00
 4.00      0.00
 4.00     -1.00
 4.00     -1.75
 4.00     -2.25
 3.50     -2.75
 2.75     -3.50
 2.25     -4.00
 1.50     -4.00
 0.75     -4.00
 0.00     -4.00
                    3
60.00      0.0     0.0      12.0      0.0      0.0     1
 0.00      4.00
 0.75      4.00
 1.50      4.00
 2.25      4.00
 2.75      3.50
 3.50      2.75
 4.00      2.25
 4.00      1.75
 4.00      1.00
 4.00      0.00
 4.00     -1.00
 4.00     -1.75
 4.00     -2.25
 3.50     -2.75
 2.75     -3.50
 2.25     -4.00
 1.50     -4.00
 0.75     -4.00
 0.00     -4.00
                    3
180.00     0.0     0.0      12.0      0.0      0.0     1     2     12    3
 0.00      4.00
 0.75      4.00
 1.50      4.00
 2.25      4.00
 2.75      3.50
 3.50      2.75
 4.00      2.25
 4.00      1.75
 4.00      1.00
 4.00      0.00
 4.00     -1.00
 4.00     -1.75
 4.00     -2.25
 3.50     -2.75
 2.75     -3.50
 2.25     -4.00
 1.50     -4.00
 0.75     -4.00
 0.00     -4.00
                    3
180.00     0.0     0.0      12.0      0.0      0.0     1
 0.00      4.00
 0.75      4.00
 1.50      4.00
 2.25      4.00
 2.75      3.50
 3.50      2.75
 4.00      2.25
 4.00      1.75
```

```
  4.00      1.00
  4.00      0.00
  4.00     -1.00
  4.00     -1.75
  4.00     -2.25
  3.50     -2.75
  2.75     -3.50
  2.25     -4.00
  1.50     -4.00
  0.75     -4.00
  0.00     -4.00

                                    3
228.00      0.0        0.0          12.0        0.0        0.0     1    5    5    3
  0.00      4.00
  0.75      4.00
  1.50      4.00
  2.25      4.00
  2.75      3.50
  3.50      2.75
  4.00      2.25
  4.00      1.75
  4.00      1.00
  4.00      0.00
  4.00     -1.00
  4.00     -1.75
  4.00     -2.25
  3.50     -2.75
  2.75     -3.50
  2.25     -4.00
  1.50     -4.00
  0.75     -4.00
  0.00     -4.00

                                    3
180.        0.0
340.
360.

                                    3    5    1
  0                              NO WAKE
                                    5
  0
```

THIS PAGE

INTENTIONALLY

LEFT BLANK

REFERENCES

1. Groves, N.C., T.T. Huang, and M.S. Chang, "Geometric Characteristics of DARPA SUBOFF Models (DTRC Models 5470 and 5471)," Report DTRC/SHD-1298-01 (1989).

2. Huang, T.T., H.L. Liu and N.C. Groves, "Experiments of DARPA SUBOFF Program," Report DTRC/SHD-1298-02 (1989).

3. Maskew, B. "Prediction of Subsonic Aerodynamic Characteristics – A Case for Low-Order Panel Methods," AIAA 19th Aerospace Sciences Meeting, Paper 81-0252, St. Louis, Missouri (January 1981).

4. Cebeci, T. and A.M.O. Smith, Analysis of Turbulent Boundary Layer, Academic Press, New York (1974).

5. Wang, H.T. and T.T. Huang, "Calculation of Potential Flow/Boundary Layer Interaction on Axisymmetric Bodies," ASME Symposium on Turbulent Boundary Layers, Niagara Falls, New York. pp. 47-57 (18-20 June 1979).

6. Bowers, B.E., "The Anechoic Flow Facility - Aerodynamic Calibration and Evaluation," SAD-48E-1942 (May 1973).